administration of anti-VEGF antibodies temporarily inhibits tumor growth by suppressing mitosis but prolonged treatment may result in more malignant behavior that includes recovery of mitosis and suppression of apoptosis.

Treatment with anti-VEGF antibodies induces intratumoral hypoxia in human colon cancer xenografts

To address the molecular events induced by anti-VEGF antibody treatment in human colon cancer xenografts, we performed DNA microarray analyses using a human gene chip. Unsupervised hierarchical clustering revealed two distinct clusters: control tumors and anti-VEGF antibody-treated tumors (Fig. 2*a*). Of the 36,079 genes analyzed, 425 genes were differentially expressed between anti-VEGF antibody-treated tumors and control tumors by 1.18-fold and with *p*-values of <0.05 (Fig. 2*a*, Supporting Information Table S1). Of these, 229 genes were higher and 196 were lower in anti-VEGF antibody-treated tumors compared with the control (Fig. 2*a*). We then utilized gene set enrichment analysis to focus on gene sets that shared common biological functions, chromosomal location and regulation.[20] Gene set enrichment analysis using 963 gene sets from the Molecular Signatures Database revealed 486 gene sets were up-regulated in the anti-VEGF antibody-treated group (Supporting Information Table S2). Of these, 37 gene sets were significantly enriched at false discovery rate of <25%, and 98 gene sets were significantly enriched at nominal *p*-value of <1%. The gene sets – HYPOXIA_REG_UP, HYPOXIA_FIBRO_UP and HIF1_TARGETS were upregulated with normalized enrichment scores of 1.66, 1.56 and 1.56, respectively, in the anti-VEGF antibody-treated group (Fig. 2*b*). These findings suggest that suppression of tumor angiogenesis caused by anti-VEGF antibody therapy induced tumor hypoxia and resulted in the activation of HIF-1 target genes.

Treatment with anti-VEGF antibodies activates HIF-1 protein

The activation of HIF-1 protein was confirmed by immunohistochemistry. HIF-1α is a transcription factor known to stabilize and translocate to the nucleus under hypoxic conditions.[21] The HIF-1α nuclear positive ratio was significantly higher in anti-VEGF antibody-treated tumors (10.24%) than in the control (4.91%) ($p = 0.01$) (Fig. 2*c*). These data support the hypothesis that intratumoral hypoxia activates HIF-1α protein and its target genes, which may then contribute to phenotypic alterations in colon cancers during anti-angiogenic therapy.

Treatment with anti-VEGF antibodies increases ALDH1-positive cells

Recent reports have uncovered the existence of cancer stem cells that could be enriched by microenvironmental cues such as chronic hypoxia, leading to enhanced malignant tumor potential.[9] To examine whether the cancer stem cell population was altered by anti-VEGF antibody treatment in our colon cancer xenograft model, immunohistochemical analyses for ALDH1, a representative marker for cancer stem cells in colorectal cancer,[22,23] were performed. The ratio of ALDH1-positive cells in anti-VEGF antibody-treated tumors was significantly higher ($3.82 \pm 1.68\%$) than in control tumors ($1.88 \pm 0.77\%$) at day 35 ($p < 0.01$) but not at day 14 (Supporting Information Fig. S3a, b). These results suggest that continuous treatment with anti-VEGF antibodies increases the number of ALDH1-positive cells, which may contribute to the enhanced malignant behavior of colon cancer xenografts.

Stanniocalcin2 is up-regulated by anti-VEGF therapy

Of the genes identified in microarray analysis, *STC2*, was the most strongly upregulated by anti-VEGF therapy (2.047-fold, Table 1). STC2 is a secreted glycoprotein hormone implicated in several human cancers, including colorectal cancer.[24] Recently, *STC2* was reported to be a direct target gene of HIF-1.[25] Therefore, we decided to examine the role of STC2 in colon cancers under hypoxic conditions. Up-regulation of STC2 mRNA in anti-VEGF antibody-treated tumors was confirmed by quantitative RT-PCR (1.618-fold, $p = 0.025$; Fig. 3*a*). STC2 protein was evaluated by immunohistochemistry and was detected in the cytoplasm of tumor cells. Consistent with mRNA levels, STC2 protein expression was higher in anti-VEGF antibody-treated tumors compared with the control (Fig. 3*b*). These findings suggest that treatment with anti-VEGF antibodies up-regulated STC2 expression at both the mRNA and protein levels.

Hypoxia up-regulates STC2 expression in human colon cancer cells

Volland *et al.* reported that overexpression of STC2 reduced proliferation of neuroblastoma cells;[26] however, Law *et al.* reported that overexpression of STC2 in SKOV3 cells, an ovarian cancer cell line, promoted cell proliferation and invasion [27]. Although STC2 has been suggested as a prognostic marker of colorectal cancer, its function in colorectal cancer remains unknown. To address the functions of STC2 in colorectal cancer, we performed *in vitro* studies using SW480 and HCT116 human colon cancer cell lines. Consistent with recent reports on other cancer cells, STC2 mRNA expression increased by 4.5-fold with hypoxia in both SW480 and HCT116 cells (Fig. 4*a*). Western blot analysis revealed that protein levels of STC2 were increased by hypoxia in SW480 cells but not in HCT116 cells (Fig. 4*b*). To address the role of HIF-1 in regulating STC2 expression under hypoxic conditions, SW480 cells were treated with siRNA against HIF-1α and incubated in hypoxic conditions. As shown in Supporting Information Fig. S4a, b, neither STC2 mRNA or protein levels changed following knockdown of HIF-1α, despite the efficient knockdown of HIF-1α protein. These findings suggest that STC2 expression increases under hypoxic conditions in a HIF-1α-independent manner.

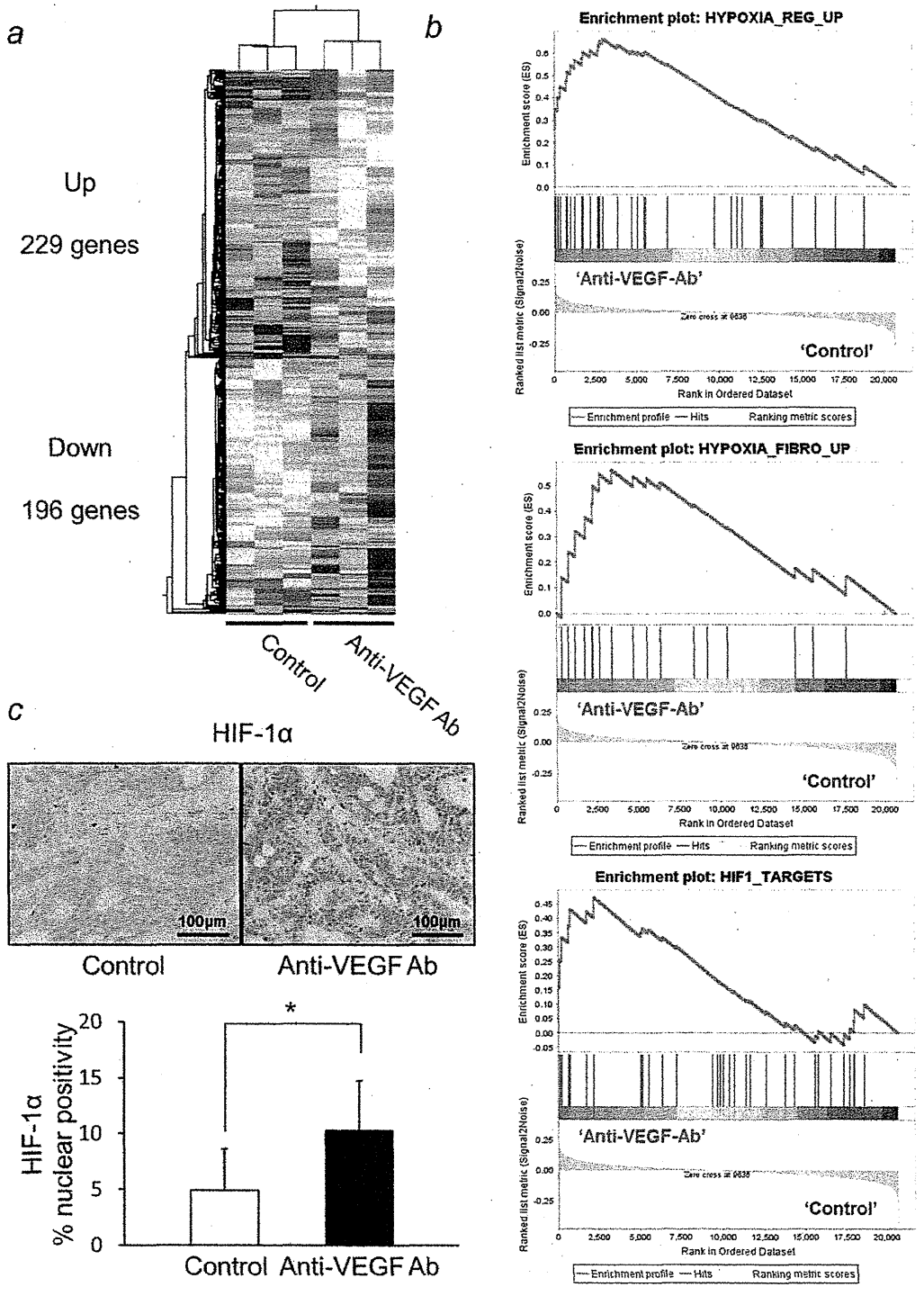

Figure 2. Microarray analysis of orthotopic human colon cancer xenografts treated with anti-VEGF antibodies or control IgG. (*a*) Unsupervised hierarchical clustering. Control tumors and anti-VEGF antibody-treated tumors were classified into distinct clusters. Of 36,079 genes analyzed, 229 and 196 genes were higher (*up*) and lower (*down*), respectively, in anti-VEGF antibody-treated tumors compared with the control. (*b*) Gene set enrichment analysis. Of 963 gene sets from the Molecular Signatures Database, 486 gene sets were up-regulated in the anti-VEGF antibody-treated group. The gene sets –HYPOXIA_REG_UP, HYPOXIA_FIBRO_UP and HIF1_TARGETS were upregulated with normalized enrichment scores of 1.66, 1.56 and 1.56, respectively, in the anti-VEGF antibody-treated group. (*c*) Immunohistochemical analysis of HIF-1α. *Upper*, representative images of immunostaining for human HIF-1α in orthotopic tumors at day 35 (×400 magnification); *lower*, quantitative evaluation of nuclear staining of HIF-1α protein in tumor cells at day 35. HIF-1α nuclear positive ratios were significantly higher in anti-VEGF antibody-treated tumors (10.24%) than that of the control (4.91%) ($p = 0.01$). Bars, SE; *, $p < 0.05$.

Table 1. Top 20 genes with significant increases in gene expression levels in anti-VEGF antibody-treated tumors

Gene symbol	Gene description	Fold change
STC2	stanniocalcin 2	2.047
RNU4-2	RNA, U4 small nuclear 2	2.019
HSPH1	Heat shock 105kDa/110kDa protein 1	1.923
LOC644714		1.913
HERPUD1	homocysteine-inducible, endoplasmic reticulum stress-inducible, ubiquitin-like domain member 1	1.875
DDIT4	DNA-damage-inducible transcript 4	1.822
		1.799
HSPA1B|HSPA1A	heat shock 70kDa protein 1B | heat shock 70kDa protein 1A	1.767
HSPA1B|HSPA1A	heat shock 70kDa protein 1B | heat shock 70kDa protein 1A	1.767
HSPA1B|HSPA1A	heat shock 70kDa protein 1B | heat shock 70kDa protein 1A	1.765
HSPA1A|HSPA1B	heat shock 70kDa protein 1A | heat shock 70kDa protein 1B	1.752
HSPA1A|HSPA1B	heat shock 70kDa protein 1A | heat shock 70kDa protein 1B	1.740
KLK10	kallikrein-related peptidase 10	1.715
CES1	carboxylesterase 1 (monocyte/macrophage serine esterase 1)	1.696
ASNS	asparagine synthetase	1.695
CHORDC1	cysteine and histidine-rich domain (CHORD)-containing 1	1.684
ID1	inhibitor of DNA binding 1, dominant negative helix-loop-helix protein	1.661
SLC7A5	solute carrier family 7 (cationic amino acid transporter, y+ system), member 5	1.644
CLIC4	chloride intracellular channel 4	1.624
GATM	glycine amidinotransferase (L-arginine:glycine amidinotransferase)	1.622

STC2 regulates growth and migration of colon cancer cells under hypoxic conditions

To gain additional insight into the molecular functions of STC2, we conducted functional assays of STC2-knockdown cells under hypoxia. First, we confirmed that two independent siRNAs, STC2-siRNA #1 and #2, efficiently depleted STC2 mRNA and protein levels in SW480 cells (Supporting Information Fig. S4c, d). Next, to assess the effects of STC2 on cell growth, a cell counting assay under hypoxic conditions was performed. SW480 cells were transfected with control siRNA or siRNA against STC2 and cultured in hypoxic conditions, and cell numbers were counted at 0, 24, 48 and 72 hr. The number of SW480 cells treated with STC2 siRNA was significantly lower than control cells at 48 and 72 hr under hypoxia (Fig. 4*c*). To address the effects of STC2-knockdown on cell migration, a scratch assay was performed. Migration of SW480 cells under hypoxic conditions was significantly inhibited by knockdown of STC2 at 48 hr (Figs. 4*d* and 4e). These results suggest that STC2 is involved in the regulation of human colon cancer cell growth and migration under hypoxic conditions. Meanwhile, cell growth was retarded but migration was not affected by knockdown of STC2 under normoxic conditions (Supporting Information Fig. S4e, f).

Long-term anti-VEGF therapy accelerates tumor regrowth *in vivo*

Because treatment with anti-VEGF antibodies promoted intratumoral hypoxia, suppressed apoptosis and upregulated STC2, we postulated that long-term administration of anti-VEGF antibodies may increase the tumorigenicity of colon cancers. To address this hypothesis, *in vivo* serial transplantation experiments were conducted using TK-4 xenografts (Supporting Information Fig. S2). Because control mice usually die from ileus about 60 days after orthotopic implantation of tumors into the cecal wall, TK-4 was instead subcutaneously implanted into nude mice and mice were treated with bevacizumab or a control antibody (5 mg/kg/day) for over 60 days. As shown in Supporting Information Fig. S5a and b, the size of subcutaneous tumors was lower in the bevacizumab-treated group than in the control after 35 days of treatment. Mice were sacrificed at 28, 56 and 84 days of treatment and subcutaneous tumors, the weight of which was significantly lower in the bevacizumab-treated group at day 56 and 84 (Fig. 5*a*), were cut into sections of equal size and orthotopically implanted into the cecal walls of secondary recipient mice (groups A, B and C, Supporting Information Fig. S2). Fifty-six days after orthotopic transplantation, mice were sacrificed and cecal tumors resected. The final weight of cecal tumors in group A was not affected by 28 days of pretreatment with bevacizumab; however, bevacizumab treatment for 56 and 84 days in groups B and C resulted in increased weights of sequentially transplanted tumors (Fig. 5*c*). Interestingly, whereas microvessel densities in tumors at transplantation were lower in bevacizumab-treated mice than in the control for groups B and C (Fig. 5*b*); those in secondary transplants were equivalent between

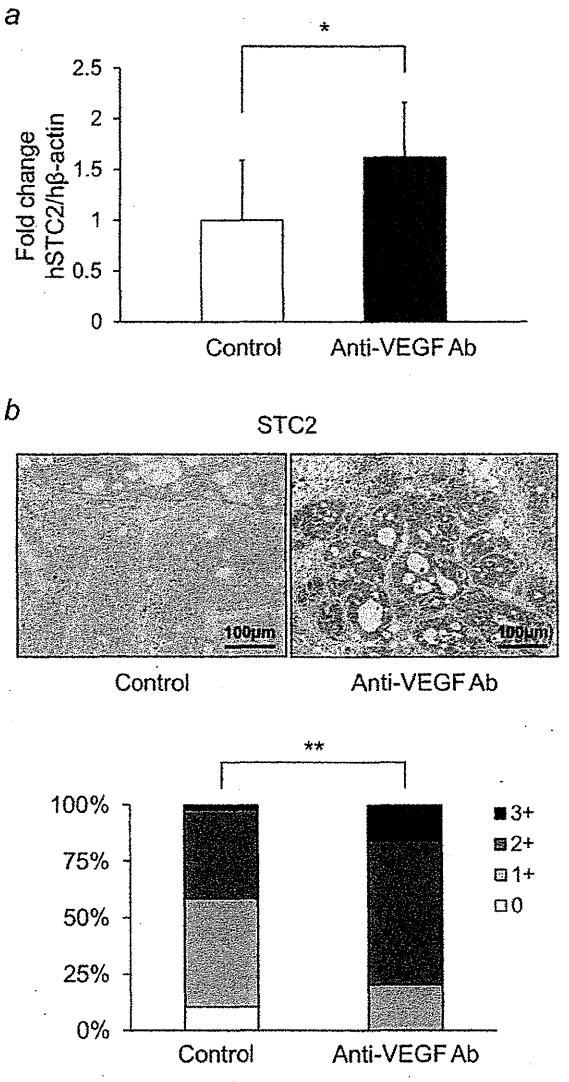

Figure 3. Effects of anti-VEGF antibody therapy on STC2 expression in orthotopic human colon cancer xenografts. (*a*) Quantitative RT-PCR (qRT-PCR) analysis of STC2. Data are normalized to internal human β-actin. mRNA levels of human STC2 (hSTC2) were higher in anti-VEGF antibody-treated tumors than in control tumors at day 35 (1.618-fold, $p = 0.025$). (*b*) Immunohistochemical analysis for hSTC2. *Upper*, representative images of immunostaining for human STC2 in cecal tumors at day 35 (×400 magnification). STC2 protein was detected in the cytoplasm of tumor cells. *Lower*, the staining intensity of STC2 was scored as 0 (none), 1+ (weak), 2+ (moderate) or 3+ (strong) in one to five randomly selected areas (×400 magnification). Expression levels of STC2 were higher in anti-VEGF antibody-treated tumors compared with the control. Bars, SE; *, $p < 0.05$.

control and bevacizumab-pretreated tumors (Fig. 5*d*). The mRNA levels of STC2 and ratio of ALDH1-positve cells in tumors at transplantation were increased in bevacizumab-treated mice for groups B and C (Supporting Information Fig. S5c, d). As tumor-stroma interaction is known to influence the malignant behavior of tumor cells, we evaluated stromal areas in subcutaneous tumors treated with bevacizumab or control IgG. Interestingly, the stromal areas in subcutaneous tumors at day 56 and 84 were larger in the bevacizumab-treated group than in the control (Supporting Information Fig. S5e). These results suggest that long-term treatment with bevacizumab increases STC2 expression, ALDH1-positive cells and tumor stroma, which may contribute to tumor cell education and increased tumorigenicity, and accelerate tumor regrowth in secondary recipient mice.

STC2 is highly expressed in human clinical colorectal liver metastasis treated with anti-VEGF antibody

To address whether anti-VEGF therapy induces STC2 in clinical colorectal cancers, we immunohistochemically analyzed STC2 protein expression levels in clinical samples of colorectal liver metastasis in patients who underwent hepatectomy after conventional chemotherapy with or without bevacizumab. STC2 expression in entire area of samples analyzed tended to be higher in colorectal liver metastases treated with bevacizumab than those without bevacizumab administration (Supporting Information Fig. S6a). Furthermore, STC2 was predominantly expressed in likely hypoxic areas around necrotic regions rather than in the peripheral area of tumors adjacent to normal liver, regardless of the preoperative use of bevacizumab (Supporting Information Fig. S6a). Thus, we quantified the necrotic area in clinical samples of colorectal liver metastases using H&E stained sections. The ratio of necrotic area was significantly higher in tumors treated with bevacizumab than those without bevacizumab treatment (31.0 *vs.* 12.0 %, $p = 0.022$, Supporting Information Fig. S6b), whereas the maximum diameters of tumors analyzed were comparable between the two groups (Supporting Information Fig. S6c). These findings suggest that anti-VEGF antibody therapy upregulated STC2 expression perhaps owing to increased hypoxic areas in human clinical colorectal liver metastasis.

Discussion

We have highlighted the phenotypic alterations that occur during continuous treatment with anti-VEGF antibodies on TK-4, a human colon cancer xenograft. Because TK-4 is a solid tumor strain derived from human colon cancer that retains its original histopathological features, our model better represents clinical colorectal cancer that generally interacts with the stroma and pathologically exhibits heterogeneity. Clinically, anti-VEGF antibodies are used for advanced or recurrent colorectal cancer patients in combination with anticancer agents, such as fluorouracil, leucovorin, irinotecan and oxaliplatin.[4,12] To exclude the specific effects of conventional chemotherapy and to uncover the effects of the anti-VEGF antibody itself, we selected a single treatment strategy in the present study. It would be interesting to examine whether molecular events induced by anti-VEGF antibodies alone can be seen when combined with chemotherapy.

As shown in Figure 1, anti-VEGF therapy inhibited tumor growth and angiogenesis; however, prolonged treatment resulted in recovery of mitosis and suppression of apoptosis. Clinically, rapid tumor regrowth after cessation of bevacizumab has been reported in patients with colorectal liver metastases and in patients with recurrent high-grade glioma.[10,28] However, continuous therapy with anti-angiogenic agents promoted revascularization in pancreatic islet tumors *via* the activation of alternative angiogenic factors such as bFGF and angiopoietin or elicited an invasive phenotype *via* the induction of tumor hypoxia.[7] In addition, anti-angiogenic agents induced intratumoral hypoxia in breast cancer xenografts, resulting in an increase in cancer stem cell populations.[9] There seem to be at least two distinct mechanisms of resistance to anti-angiogenic therapy:[29] (*i*) sustainment of angiogenesis or revascularization *via* alternative angiogenic processes; and (*ii*) increases in the malignant behavior of tumor cells caused by an alteration in the tumor microenvironment. Intratumoral hypoxia appears to play important roles in both mechanisms. In this study, angiogenesis was suppressed over time in tumors treated with anti-VEGF antibodies. In microarray analysis, genes regulated by hypoxia were upregulated. Most of the phenotypic alterations and molecular events seen in our experiments could be induced by intratumoral hypoxia and appear to be related with the latter mechanism mentioned earlier.

STC2 is a secreted glycoprotein hormone and its receptor remains unknown. It is thought that STC2 functions in a paracrine or an autocrine manner.[30] STC2 is reported to be involved in human cancers[30,31] and proposed to be a prognostic marker for renal, breast, castration-resistant prostate, gastric, esophageal and colorectal cancer.[24,32–35] STC2 expression is stimulated by hypoxia and/or unfolded protein responses in human cancers.[36,37] Recent *in vitro* evidence support the notion that STC2 is associated with aggressive cancer phenotypes in ovarian, breast and hepatocellular carcinoma.[25,27,38] Furthermore, it has been reported that human *STC2* is a HIF-1 target gene and the upregulation of STC2 expression stimulated growth of human ovarian and breast cancer cells (for example, SKOV3 and MCF7) under hypoxic conditions.[25] However, the roles of STC2 under hypoxic conditions in colorectal cancer are unknown.

In this study, mRNA expression of STC2 increased under hypoxia in two colon cancer cell lines, SW480 and HCT116, consistent with previous reports of other cancer cell lines.[25] In contrast, the expression levels of STC2 protein increased under hypoxia in SW480 but not HCT116 cells. Because STC2 is a secreted protein, the protein levels in cell lysates may not necessarily reflect the total amount of STC2 produced in cells. Interestingly, HIF-1α knockdown did not affect STC2 expression in SW480 cells. Because STC2 is an unfolded protein response target as well as a HIF-1 target and hypoxic stress itself could induce STC2, depletion of HIF-1 alone may be insufficient to suppress STC2 in our *in vitro* experiments. We demonstrated that STC2 in SW480 cells exhibited a growth advantage under hypoxia. Furthermore, it has been reported that overexpression of STC2 resulted in an invasive phenotype in hypoxic SKOV3 cells through induction of an epithelial-mesenchymal transition (EMT) program.[27] Although we have not tested whether hypoxic SW480 cells undergo EMT with or without STC2 knockdown, SW480 cell migration was inhibited by STC2 knockdown under hypoxia. These results suggest that STC2 confers a growth and migratory advantage under hypoxia. Meanwhile, in normoxic condition, cell growth was retarded but migration was not affected by STC2 knockdown. The difference in the function of STC2 between normoxia and hypoxia requires further investigation.

To test whether continuous anti-VEGF treatment affects tumorigenicity, a serial transplantation model was employed in which subcutaneous implantation of TK-4 in primary mice enabled long-term treatment with bevacizumab. We recently observed that tumor microenvironments differ between subcutaneous and orthotopic xenograft sites.[13] In this study, STC2 mRNA expression was upregulated by bevacizumab treatment even in subcutaneous tumors. Therefore, this serial transplantation model seems reasonable for the analysis of the tumor microenvironment, at least when focusing on STC2 alteration. As a result, long-term blockade of VEGF by bevacizumab increased the tumorigenicity of colon cancer xenografts in secondary recipient mice. The stromal areas in tumors at transplantation were larger in the bevacizumab-treated group than in the control. Bevacizumab is specific for human VEGF and does not neutralize the stromal-derived murine VEGF. The stroma in PDX models consist primarily of murine fibroblasts that might produce considerable VEGF under hypoxic conditions. In this study, microvessel densities were equivalent between control and bevacizumab-pretreated tumors in secondary recipient mice. The possibility that elevated growth of secondary transplants was because of the production of murine VEGF under continuous pressure by bevacizumab appears to be ruled out.

A number of studies suggest that the cancer stem cell phenotype can be enhanced by microenvironmental influences.[39,40] In recent reports, anti-angiogenic agents increased the population of cancer stem cells *via* the generation of hypoxia in human breast cancer xenografts.[9] Furthermore, cancer stem cells, with their capability for tumorigenicity and self-renewal, are believed to mediate cancer relapse after chemotherapy.[41] The concept that colon cancer stem cells can be identified through the expression of CD133 and other markers, such as epithelial-specific antigen, CD44, CD166, Musashi-1, CD29, CD24, leucine-rich repeat-containing G-protein-coupled receptor 5 and ALDH1, has been proposed.[23] In this study, ALDH1-positive cells increased during anti-VEGF treatment in both orthotopic and subcutaneous implantation models. In our serial transplantation model, pretreatment of subcutaneous tumors with bevacizumab in primary mice accelerated the growth of tumors orthotopically transplanted into the cecal wall of secondary mice. It seems that tumorigenic capacity was enhanced by

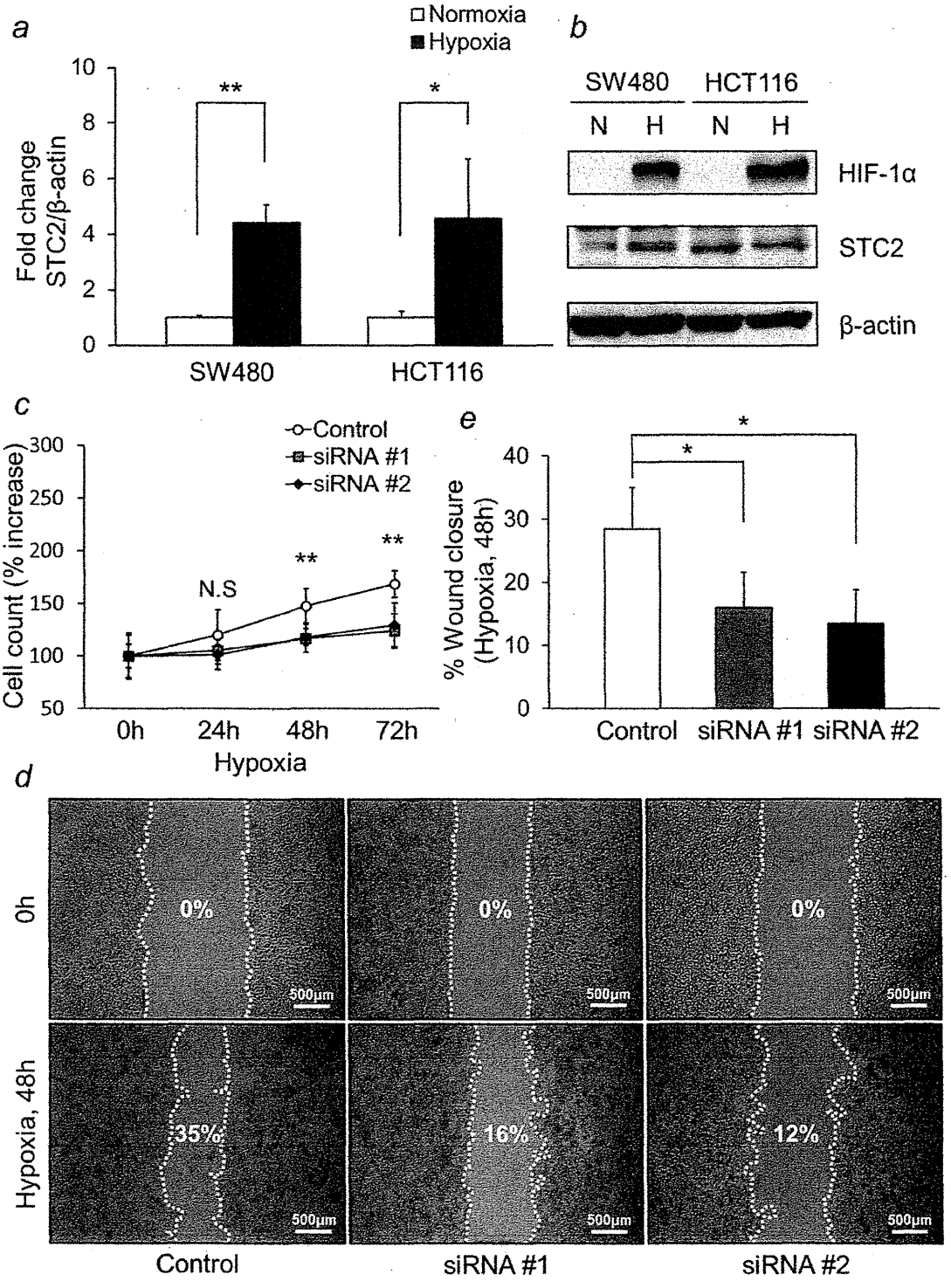

Figure 4. *In vitro* functional analyses of STC2 in colon cancer cells. (*a, b*) Hypoxic induction of STC2. SW480 and HCT116 cells were incubated under hypoxic conditions for 12 hr and STC2 mRNA and protein levels were analyzed by qRT-PCR (*a*) and western blotting (*b*), respectively. STC2 mRNA levels were increased 4.5-fold by hypoxia in both SW480 and HCT116 cells. STC2 protein levels were increased by hypoxia in SW480 cells but not in HCT116 cells. (*c*) Cell counting assay under hypoxic conditions. SW480 cells were transfected with control siRNA or two independent siRNAs against STC2 and cultured under hypoxic conditions; cell numbers were counted at 0, 24, 48 and 72 hr. The number of SW480 cells treated with STC2 siRNA was significantly lower than control cells at 48 and 72 hr. (*d, e*) Scratch assay under hypoxic conditions. SW480 cells were transfected with control siRNA or two independent siRNAs against STC2. After cultured in normoxia for 36 hr, scratches were made on the slides and cells were incubated under hypoxic conditions for 48 hr. Photographs were taken using a light microscope (*d*) and wound closure was evaluated using ImageJ software and calculated as [area of gap (0 hr) – area of gap (48 hr)]/area of gap (0 hr) × 100 (*e*). Migration of SW480 cells under hypoxic condition was significantly inhibited by STC2 knockdown . Bars, SE; *, $p < 0.05$; **, $p < 0.01$; N.S, not significant.

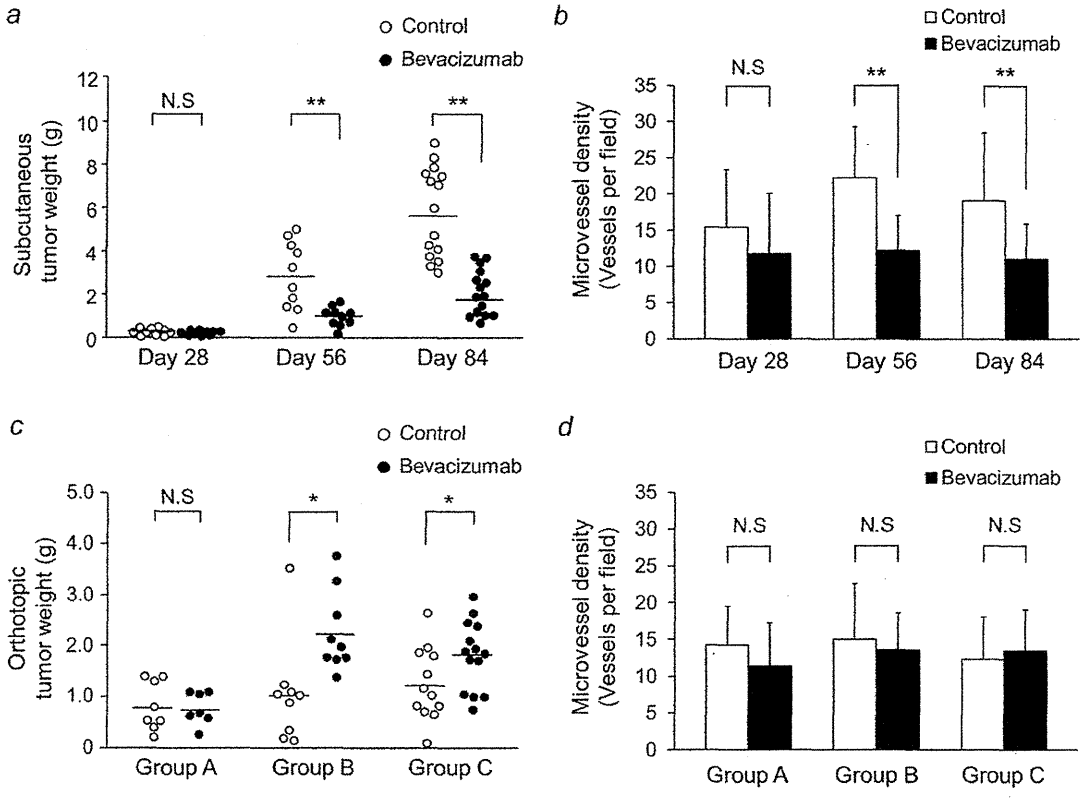

Figure 5. Effects of long-term administration of anti-VEGF antibodies on tumorigenicity of colon cancers xenografts in the *in vivo* serial implantation model. TK-4 was subcutaneously implanted into nude mice and treated with bevacizumab or control antibodies (5 mg/kg/day) for 84 days. (*a*) Weight of subcutaneous tumors in control and bevacizumab-treated mice at day 28, 56 and 84. Tumor weight was lower in the bevacizumab-treated group than in the control at day 56 and 84. (*b*) Mice were sacrificed at days 28, 56 and 84 and subcutaneous tumors were resected. Microvessel densities in subcutaneous tumors were lower in bevacizumab-treated mice than in the control at days 56 and 84. (*c*) Subcutaneous tumors resected at days 28, 56 and 84 were cut into sections of equal size and orthotopically implanted into the cecal walls of secondary recipient mice (groups A, B and C, see Supporting Information Fig. S2). Fifty-six days after orthotopic transplantation, mice were sacrificed and cecal tumors were resected. Final weights of cecal tumors in group A were not affected by 28 days of pretreatment with bevacizumab; however, bevacizumab treatment for 56 and 84 days in groups B and C resulted in increased weight of transplanted tumors at the cecal walls of secondary mice. (*d*) Quantitative evaluation of microvessel densities (average of five high-power fields) in cecal tumors of secondary recipient mice. No difference was observed between control tumors and bevacizumab-pretreated tumors in group A, B and C. Bars, SE; *, $p < 0.05$; **, $p < 0.01$; N.S, not significant.

long-term treatment with anti-VEGF antibodies, which may be in part caused by an increased population of ALDH1-positive cancer stem cells. In subcutaneous tumors treated with bevacizumab, the area of tumor stroma was increased after 56 days, which may potentially increase the number of cancer stem cells and enhance their malignant potential.

Finally, immunohistochemical analysis revealed that STC2 protein was predominantly expressed in likely hypoxic areas around necrotic regions in clinical samples of colorectal liver metastasis in patients treated with or without bevacizumab before hepatectomy. In addition, the ratio of necrotic area was significantly higher in colorectal liver metastasis treated with bevacizumab, consistent with a previous report by Loupakis *et al.*[42] These findings suggest that anti-VEGF antibody therapy induces intratumoral hypoxia leading to upregulation of STC2, which may increase the malignant potential of persistent tumor cells. It seems difficult to define the resistance to anti-VEGF antibody in a clinical setting, because colorectal cancer patients are rarely treated with bevacizumab alone but usually in combination with conventional chemotherapy, and failure of such treatments is recognized as resistant to chemotherapy. However, intratumoral hypoxia induced by anti-VEGF antibody therapy appears to enhance the malignant potential of colorectal cancers and contribute to treatment failure.

Taken together, our data provide a potential explanation for the limited clinical effectiveness of anti-angiogenic agents and possible rebound phenomenon after withdrawal of bevacizumab. If this is the case, then improving the clinical efficacy of anti-angiogenic treatments will require the concurrent use of cancer stem cell-targeting agents. Moreover, a proper window of duration of anti-angiogenic therapy should be designed to avoid generation of intratumoral hypoxia.

In conclusion, we have identified phenotypic alterations and molecular events induced by anti-VEGF antibody therapy in a colon cancer xenograft model. Intratumoral hypoxia appears to play an important role in regulating multiple processes that increase the cancer stem cell population and accelerate the malignant potential of colon cancers. STC2 can be induced by hypoxia to enhance colon cancer cell growth and migration. Long-term administration of anti-VEGF antibodies increases the tumorigenicity of colon cancers and accelerates tumor growth when transplanted into secondary recipient mice. These data provide a potential explanation for the limited clinical effectiveness of anti-angiogenic agents and rebound phenomenon after withdrawal of bevacizumab.

Acknowledgements

The authors thank Chugai Pharmaceutical Co. for providing bevacizumab, Dr. Daniel C. Chung at Massachusetts General Hospital for reading the manuscript and giving helpful suggestions, and Dr. Takanori Sakaguchi and other laboratory members for their helpful discussions. Grant support by Ministry of Education, Culture, Sports, Science and Technology of Japan Grants-in-aid 22791270 (H. Kikuchi), 24591937 (H. Kikuchi), 22300329 (M. Kitagawa) and 24390312 (H. Konno).

References

1. Cunningham D, Atkin W, Lenz HJ, et al. Colorectal cancer. *Lancet* 2010;375:1030–47.
2. Folkman J. Angiogenesis in psoriasis: therapeutic implications. *J Invest Dermatol* 1972;59: 40–3.
3. Donnem T, Hu J, Ferguson M, et al. Vessel co-option in primary human tumors and metastases: an obstacle to effective anti-angiogenic treatment? *Cancer Med* 2013;2:427–36.
4. Hurwitz H, Fehrenbacher L, Novotny W, et al. Bevacizumab plus irinotecan, fluorouracil, and leucovorin for metastatic colorectal cancer. *New Eng J Med* 2004;350:2335–42.
5. Ellis LM, Hicklin DJ. VEGF-targeted therapy: mechanisms of anti-tumour activity. *Nat Rev Cancer* 2008;8:579–91.
6. Nazer B, Humphreys BD, Moslehi J. Effects of novel angiogenesis inhibitors for the treatment of cancer on the cardiovascular system: focus on hypertension. *Circulation* 2011;124:1687–91.
7. Casanovas O, Hicklin DJ, Bergers G, Hanahan D. Drug resistance by evasion of antiangiogenic targeting of VEGF signaling in late-stage pancreatic islet tumors. *Cancer Cell* 2005;8:299–309.
8. Pàez-Ribes M, Allen E, Hudock J, et al. Antiangiogenic therapy elicits malignant progression of tumors to increased local invasion and distant metastasis. *Cancer Cell* 2009;15:220–31.
9. Conley SJ, Gheordunescu E, Kakarala P, et al. Antiangiogenic agents increase breast cancer stem cells *via* the generation of tumor hypoxia. *Proc Natl Acad Sci* 2012;109: 2784–9.
10. Cacheux W, Boisserie T, Staudacher L, et al. Reversible tumor growth acceleration following bevacizumab interruption in metastatic colorectal cancer patients scheduled for surgery. *Ann Oncol* 2008;19:1659–61.
11. Miles D, Harbeck N, Escudier B, et al. Disease course patterns after discontinuation of bevacizumab: pooled analysis of randomized phase III trials. *J Clin Oncol* 2011;29:83–8.
12. Davies JM, Goldberg RM. Treatment of metastatic colorectal cancer. *Sem Oncol* 2011;38:552–60.
13. Yamamoto M, Kikuchi H, Ohta M, et al. TSU68 prevents liver metastasis of colon cancer xenografts by modulating the premetastatic niche. *Cancer Res* 2008;68:9754–62.
14. Shoji T, Konno H, Tanaka T, et al. Orthotopic implantation of a colon cancer xenograft induces high expression of cyclooxygenase-2. *Cancer Lett* 2003;195:235–41.
15. Tanaka T, Konno H, Matsuda I, et al. Prevention of hepatic metastasis of human colon cancer by angiogenesis inhibitor TNP-470. *Cancer Res* 1995; 55:836–9.
16. Konno H, Tanaka T, Matsuda I, et al. Comparison of the inhibitory effect of the angiogenesis inhibitor, TNP-470, and mitomycin C on the growth and liver metastasis of human colon cancer. *Int J Cancer J Int du cancer* 1995;61:268–71.
17. Kikuchi H, Pino MS, Zeng M, et al. Oncogenic KRAS and BRAF differentially regulate hypoxia-inducible factor-1 and −2 in colon cancer. *Cancer Res* 2009;69:8499–506.
18. Weidner N, Semple JP, Welch WR, et al. Tumor angiogenesis and metastasis–correlation in invasive breast carcinoma. *New Eng J Med* 1991;324: 1–8.
19. Mahy P, De Bast M, Gallez B, et al. In vivo colocalization of 2-nitroimidazole EF5 fluorescence intensity and electron paramagnetic resonance oximetry in mouse tumors. *Radiotherapy Oncol* 2003;67:53–61.
20. Subramanian A. Gene set enrichment analysis: a knowledge-based approach for interpreting genome-wide expression profiles. *Proc Natl Acad Sci* 2005;102:15545–50.
21. Majmundar AJ, Wong WJ, Simon MC. Hypoxia-inducible factors and the response to hypoxic stress. *Mol Cell* 2010;40:294–309.
22. Huang EH, Hynes MJ, Zhang T, et al. Aldehyde dehydrogenase 1 is a marker for normal and malignant human colonic stem cells (SC) and tracks SC overpopulation during colon tumorigenesis. *Cancer Res* 2009;69:3382–9.
23. Todaro M, Francipane MG, Medema JP, et al. Colon cancer stem cells: promise of targeted therapy. *Gastroenterology* 2010;138:2151–62.
24. Ieta K, Tanaka F, Yokobori T, et al. Clinicopathological significance ofstanniocalcin 2gene expression in colorectal cancer. *Int J Cancer* 2009;125: 926–31.
25. Law AY, Wong CK. Stanniocalcin-2 is a HIF-1 target gene that promotes cell proliferation in hypoxia. *Exp Cell Res* 2010;316:466–76.
26. Volland S, Kugler W, Schweigerer L, et al. Stanniocalcin 2 promotes invasion and is associated with metastatic stages in neuroblastoma. *Int J Cancer* 2009;125:2049–57.
27. Law AYS, Wong CKC. Stanniocalcin-2 promotes epithelial–mesenchymal transition and invasiveness in hypoxic human ovarian cancer cells. *Exp Cell Res* 2010;316:3425–34.
28. Zuniga RM, Torcuator R, Jain R, et al. Rebound tumour progression after the cessation of bevacizumab therapy in patients with recurrent high-grade glioma. *J Neurooncol* 2010;99:237–42.
29. Bergers G, Hanahan D. Modes of resistance to anti-angiogenic therapy. *Nat Rev Cancer* 2008;8: 592–603.
30. Yeung BHY, Law AYS, Wong CKC. Evolution and roles of stanniocalcin. *Mol Cell Endocrinol* 2012;349:272–80.
31. Chang AC, Jellinek DA, Reddel RR. Mammalian stanniocalcins and cancer. *Endocr Relat Cancer* 2003;10:359–73.
32. Meyer H-A, Tölle A, Jung M, et al. Identification of Stanniocalcin 2 as prognostic marker in renal cell carcinoma. *Eur Urol* 2009;55:669–78.
33. Joensuu K, Heikkila P, Andersson LC. Tumor dormancy: elevated expression of stanniocalcins in late relapsing breast cancer. *Cancer Lett* 2008; 265:76–83.
34. Tamura K, Furihata M, Chung S-Y, et al. Stanniocalcin 2 overexpression in castration-resistant prostate cancer and aggressive prostate cancer. *Cancer Sci* 2009;100: 914–9.
35. Yokobori T, Mimori K, Ishii H, et al. Clinical significance of stanniocalcin 2 as a prognostic marker in gastric cancer. *Ann Surg Oncol* 2010; 17:2601–7.
36. Law AYS, Lai KP, Ip CKM, et al. Epigenetic and HIF-1 regulation of stanniocalcin-2 expression in human cancer cells. *Exp Cell Res* 2008;314:1823–30.
37. Ito D, Walker JR, Thompson CS, et al. Characterization of Stanniocalcin 2, a novel target of the mammalian unfolded protein response with cytoprotective properties. *Mol Cell Biol* 2004;24:9456–69.
38. Wang H, Wu K, Sun Y, et al. STC2 is upregulated in hepatocellular carcinoma and promotes cell proliferation and migration in vitro. *BMB Rep* 2012;45:629–34.
39. Lin Q, Yun Z. Impact of the hypoxic tumor microenvironment on the regulation of cancer stem cell characteristics. *Cancer Biol Ther* 2010;9: 949–56.
40. Filatova A, Acker T, Garvalov BK. The cancer stem cell niche(s): the crosstalk between glioma stem cells and their microenvironment. *Biochimica et biophysica acta* 2013;1830: 2496–508.
41. Clevers H. The cancer stem cell: premises, promises and challenges. *Nat Med* 2011;17: 313–9.
42. Loupakis F, Schirripa M, Caparello C, et al. Histopathologic evaluation of liver metastases from colorectal cancer in patients treated with FOLFOXIRI plus bevacizumab. *Brit J Cancer* 2013; 108:2549–56.

Genes to Cells

YB1 binds to and represses the *p16* tumor suppressor gene

Yojiro Kotake[1]*, Yuichi Ozawa[2], Masanori Harada[2,3], Kyoko Kitagawa[3], Hiroyuki Niida[3], Yasutaka Morita[1], Kenji Tanaka[1], Takafumi Suda[2] and Masatoshi Kitagawa[3]

[1]*Department of Biological and Environmental Chemistry, Faculty of Humanity-Oriented Science and Engineering, Kinki University, 11-6 Kayanomori, Iizuka, Fukuoka 820-8555, Japan*

[2]*Second Division, Department of Internal Medicine, Hamamatsu University School of Medicine, 1-20-1 Handayama, Higashi-ku, Hamamatsu, Shizuoka 431-3192, Japan*

[3]*Department of Molecular Biology, Hamamatsu University School of Medicine, 1-20-1 Handayama, Higashi-ku, Hamamatsu, Shizuoka 431-3192, Japan*

Y box binding protein 1 (YB1) has multiple functions associated with drug resistance, cell proliferation and metastasis through transcriptional and translational regulation. Increased expression of YB1 is closely related to tumor growth and aggressiveness. We showed that YB1 protein levels were decreased through replicative and premature senescence and were correlated with increased expression levels of $p16^{INK4A}$ tumor suppressor gene. Depletion of *YB1* was associated with increased levels of *p16* in human and murine primary cells. Forced expression of YB1 in mouse embryonic fibroblasts resulted in decreased expression of *p16* and increased cell proliferation. Senescence-associated expression of β-galactosidase was repressed in YB1-over-expressing cells. Chromatin immunoprecipitation assays showed that YB1 directly associates with the *p16* promoter. Taken together, all our findings indicate that YB1 directly binds to and represses *p16* transcription, subsequently resulting in the promotion of cell growth and prevention of cellular senescence.

Introduction

Y box binding protein 1 (YB1) is a member of the cold shock domain (CSD) protein family. This protein binds to DNA and/or RNA through the CSD and is involved in both transcriptional activation and repression by binding to the Y box elements of the target gene promoter (Kohno *et al.* 2003). YB1 is also known to play multiple roles in DNA repair, translation and RNA stabilization (Kohno *et al.* 2003). Clinical studies have shown that YB1 is expressed at high levels in a wide range of human cancers, including lung, breast, prostate and colon cancers (Bargou *et al.* 1997; Shibao *et al.* 1999; Gu *et al.* 2001; Shibahara *et al.* 2001; Gimenez-Bonafe *et al.* 2004). Increased YB1 levels are strongly associated with the expression of epidermal growth factor receptor (EGFR), HER-2 (Fujii *et al.* 2008; Lee *et al.* 2008) and CDC6 (Basaki *et al.* 2010) proteins in breast cancer.

Communicated by: Keiichi Nakayama
**Correspondence:* ykotake@fuk.kindai.ac.jp

Biochemical studies have showed that YB1 directly binds to the promoters of certain genes, including *EGFR*, *HER-2* and *CDC6*, activating their expression (Wu *et al.* 2006; Basaki *et al.* 2010); this in turn leads to increased cell growth. YB1 has also been shown to be associated with drug resistance, by binding to and activating the multidrug resistance 1 (MDR1) protein in human cancer cells (Asakuno *et al.* 1994; Ohga *et al.* 1996). Studies in mice showed the role of YB1 in cell proliferation. Transgenic mice expressing human YB1 in mammary epithelia develop breast carcinomas with mitotic failure and centrosome amplification (Bergmann *et al.* 2005). For mice, the absence of *YB1* can be embryonically lethal or lead to exencephaly (Lu *et al.* 2005; Uchiumi *et al.* 2006). $YB1^{-/-}$ mouse embryonic fibroblasts (MEFs) show retarded cell growth and are less responsive to oxidative, genotoxic and oncogenic stressors compared with their wild-type counterparts. Induction of cellular senescence by oxidative stress is enhanced in $YB1^{-/-}$ MEFs and is partly achieved by the increased mRNA expression of the cyclin-dependent kinase (CDK) inhibitors *p16* and *p21* (Lu *et al.* 2005). Basaki *et al.* have also

DOI: 10.1111/gtc.12093

showed that expression levels of p21 and p16 were increased when they were treated with YB-1 short interfering RNAs (siRNAs) in the MCF-7 human breast adenocarcinoma cell line (Basaki *et al.* 2010).

For cells entering the cell cycle, a mitogenic signal induces the expression of cyclin Ds, which bind to and activate CDK4/CDK6. This leads to inactivation of the pRB family of proteins through phosphorylation, causing pRB-E2F dissociation and promoting the cell cycle (Cobrinik 2005). Inhibition of CDK4/CDK6 activity by *p16*, which allows for the pRB family of proteins to be activated, contributes to cell cycle arrest (Serrano *et al.* 1993). The biochemical activity of p16 suggests that the protein functions as a tumor suppressor. The *p16* gene is frequently mutated, or its expression silenced in human cancers (Ruas & Peters 1998; Sharpless 2005). Mice lacking *p16* are prone to spontaneous and induced tumorigenesis (Krimpenfort *et al.* 2001; Sharpless *et al.* 2001). The expression of p16 is undetectable during embryogenesis and in young tissues. Levels of p16 protein increase with age and contribute to irreversible growth arrest known as replicative senescence (Gil & Peters 2006). Expression of *p16* is also activated by a variety of oncogenes, leading to stable cell cycle arrest, termed 'premature senescence'; this protects cells from hyperproliferative stimulation (Serrano *et al.* 1997). The *p16* locus is histone H3 lysine 27 (H3K27)-trimethylated and epigenetically repressed by polycomb repression complex 1 (PRC1) and PRC2 (Bracken *et al.* 2007; Kotake *et al.* 2007, 2009). It was recently reported that a long noncoding RNA, *ANRIL*, is required for the recruitment of PRC1 and PRC2 to the *p16* locus (Yap *et al.* 2010; Kotake *et al.* 2011). Ohtani *et al.* previously reported that the Ets2 transcription factor binds to and activates *p16*, leading to cellular senescence (Ohtani *et al.* 2001). Apart from Ets2, it is unclear which other transcription factors bind to and regulate *p16* activity. In this study, we investigated the involvement of YB1 in repressing *p16* transcription.

Results

YB1 protein levels were decreased during replicative and premature senescence

Previous studies in mice have shown that deletion of *YB1* enhances premature senescence of MEFs via oxidative stress (Lu *et al.* 2005); therefore, we suggested that YB1 may have an important role in cellular senescence. We determined the levels of expression of YB1 in response to the oncogenic Ras signal as this is known to cause premature senescence by activating *p16* transcription. MEFs ectopically expressing oncogenic Ras^{G12V} were established after retroviral transduction and used to examine the expression of YB1. Our Western blotting results indicated that p16 levels were increased by Ras^{G12V} transduction in MEFs. In contrast, YB1 levels were decreased by Ras^{G12V} transduction (Fig. 1A). Our qRT-PCR analysis showed that *YB1* mRNA levels were unaffected by Ras^{G12V} transduction (Fig. 1B).

We next examined the expression of YB1 in replicative senescence. Levels of p16 protein increased during *in vitro* passage of MEFs and contributed in part to replicative senescence. Concomitant with the increase in p16 levels, the amount of YB1 was decreased in a passage-dependent manner (Fig. 1C), whereas YB1 mRNA levels remained unchanged (Fig. 1D). Our data indicate that YB1 expression is post-transcriptionally down-regulated through both replicative and premature senescence and that reduction in YB1 levels is associated with an increase in p16 expression, suggesting that YB1 negatively regulates p16.

Silencing YB1 increases p16 gene expression in mice and humans

To examine whether YB1 is involved in the regulation of p16 expression, we knocked down mouse *YB1* using specific siRNAs in MEFs. These siRNAs reduced YB1 levels such that they were almost undetectable (Fig. 2A). Associated with the reduction in YB1 levels was a substantial increase in mouse p16 (Fig. 2A). Our qRT-PCR analysis showed that silencing *YB1* resulted in a twofold increase in *p16* mRNA (Fig. 2B). Unexpectedly, the level of protein corresponding to p21 was actually decreased by *YB1* silencing, although p21 protein expression was increased in MEFs where there was homozygous deletion of *YB1* (Lu *et al.* 2005). The INK4 locus encodes three tumor suppressor genes, *p16*, *ARF* and *p15* (a CDK inhibitor) (Gil & Peters 2006; Kim & Sharpless 2006; Sherr 2006). Transcription of the *p16-ARF-p15* gene cluster is coordinately repressed by PRC1 and PRC2 (Bracken *et al.* 2007; Kotake *et al.* 2007). Therefore, we examined whether YB1 is also involved in the regulation of p15 and Arf. Our qRT-PCR and Western blotting analyses showed that p15 and Arf levels were unaffected by the silencing of *YB1* (Fig. 2A and 2B). To confirm this, we transfected WI38 cells with human *YB1*-specific siRNAs and observed that depletion of YB1 correlated

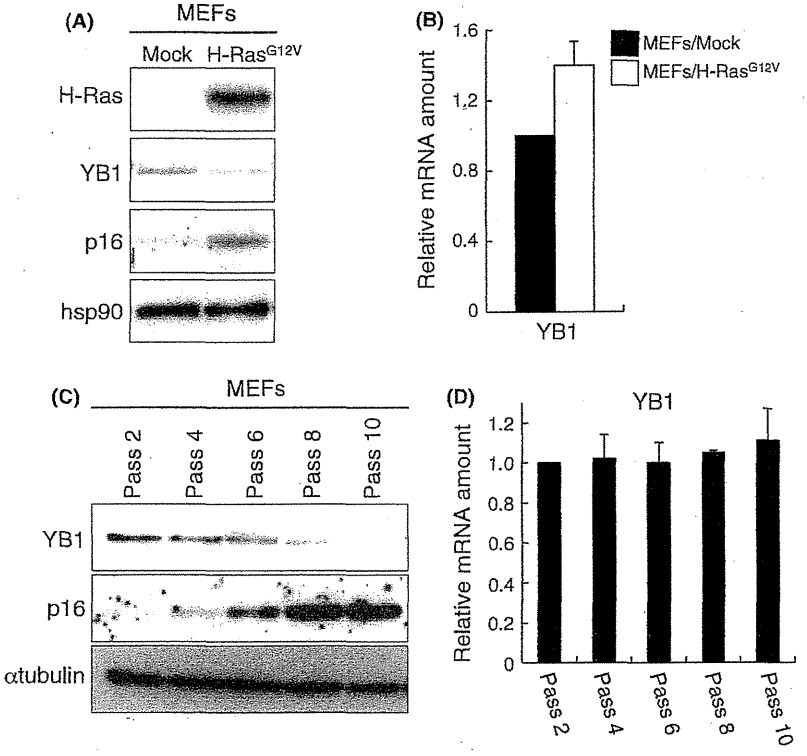

Figure 1 Inverse correlation between the levels of YB1 and p16 expression in mouse embryonic fibroblasts (MEFs). (A) MEFs were infected with control (Mock) or H-Ras^{G12V}-expressing retroviruses and selected for using puromycin. The levels of individual protein were determined by Western blotting. (B) *YB1* mRNA levels were determined by qRT-PCR, and results were expressed relative to the corresponding values for MEFs that were mock-infected. Mean values and standard deviations were calculated from triplicates of a representative experiment. (C) Passage-dependent expression of YB1 and p16 in MEFs was determined by Western blotting. (D) *YB1* mRNA levels were determined by qRT-PCR, and results were expressed relative to the corresponding values for passage 2 MEFs.

with increased expression of human p16, but not of p15, p21 and ARF (Fig. 2C and D). Our results suggest that YB1 is involved in p16 repression in both mouse and human cells.

YB1 represses p16 expression by binding to its promoter

We next examined conversely how forced expression of YB1 affects *p16* expression. MEFs stably expressing YB1 were established with the aid of YB1-expressing retroviruses. Through the qRT-PCR assays, we showed that *p16* mRNA levels in the virus-infected MEFs were substantially decreased to almost 35% of that in cells infected with control virus (Fig. 3A). Consistent with the decrease in mRNA levels, the amount of p16 protein was also decreased substantially (Fig. 3B). Associated with this, forced expression of YB1 increased the rate of proliferation for the MEFs (Fig. 3C) and corresponded to a decrease in the number of cells that stained positive for SA-β-Gal activity, an indicator of cellular senescence (Fig. 3D and E). Taken together, these data indicate that YB1 represses *p16* transcription and prevents cellular senescence.

Given that YB1 is a transcription factor, we next examined whether YB1 binds to the *p16* promoter. To clarify this issue, we carried out ChIP assay using oligonucleotide primers designed corresponding to a sequence within mouse *p16* promoter region. Sixteen putative YB-1 responsive elements were identified within the first 2.5 kb of mouse *p16* promoter (Fig. 4A). A ChIP assay showed that an anti-YB-1 antibody was able to precipitate DNA that was amplified with primer sets covering a region smaller than 1.5 kb of the mouse *p16* promoter (Fig. 4B and Fig. S1 in Supporting Information). This would suggest that YB1 directly binds to the mouse *p16* promoter.

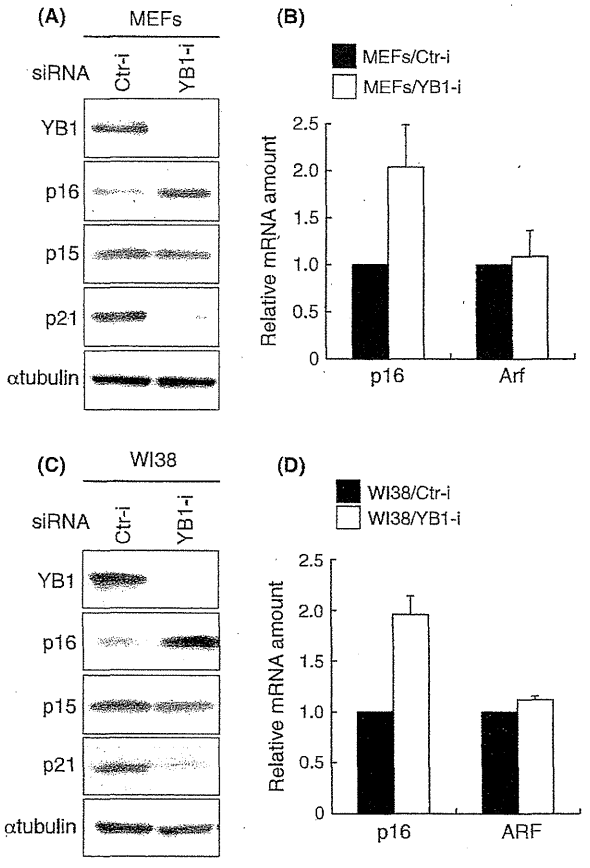

Figure 2 Silencing *YB1* resulted in an increase in *p16* mRNA levels, but not in *p15* or *ARF* mRNA transcripts. (A) MEFs were transfected with siRNAs specific for *YB1* or a control (ctr) siRNA. *YB1* silencing efficiency and the effects of silencing on p16, p15 and p21 expression were determined by Western blotting. (B) Levels of *p16* and *Arf* mRNA transcripts were determined by qRT-PCR. (C, D) WI38 cells were transfected with siRNAs specific for *YB1* or a control (ctr) siRNA. *YB1* silencing efficiency and the effects of silencing on p16, p15, p21 and ARF expression were determined by Western blotting (C) and qRT-PCR (D).

Discussion

In this study, we have outlined that YB1 is involved in the repression of *p16* transcription and cellular senescence. We observed that YB1 protein levels, but not the corresponding mRNA, were decreased during replicative and premature senescence, suggesting that YB1 is post-transcriptionally down-regulated through cellular senescence. Sorokin *et al.* previously reported that genotoxic stress induces a 20S proteasome-mediated cleavage of YB1 (Sorokin *et al.* 2005). However, we were unable to detect an increase in the occurrence of YB1 cleavage during cellular senescence (data not shown). It is possible that there are additional regulatory mechanisms involved with YB1 expression, such as ubiquitin–proteasome pathways and translational regulation.

We also found that p16 is a novel target of YB1 in both mouse and human cells. Reducing YB1 levels resulted in increased *p16* mRNA levels, but not in increases in *p15* and *ARF* mRNA levels. All these events occurred in both MEFs and WI38 cells, indicating that YB-1 specifically regulates the *p16* gene at the INK4 locus. Additionally, our ChIP data show that YB1 binds to the *p16* promoter, indicating direct regulation of *p16* by YB1. Detailed biochemical mechanisms underlying the function of YB1 during *p16* repression remain to be elucidated. PRC1 and PRC2 have been identified as repressors of *p16* transcription through histone methylation (Bracken *et al.* 2007; Kotake *et al.* 2007, 2009). The binding of these to the *p16* locus is limited during *in vitro* passage and through oncogenic signaling, which results in *p16* activation. The functional relationship between YB1 and PRC1 and/or PRC2 during *p16* repression is an important issue that requires further investigation.

YB1 is thought to be a key regulator of cell proliferation and an oncoprotein. Several genes targeted by YB1, such as p21, CDC6, EGFR and HER-2, are cell cycle regulators (Okamoto *et al.* 2000; Wu *et al.* 2006; Fujii *et al.* 2008; Lee *et al.* 2008; Basaki *et al.* 2010). Many studies have shown that increased expression of YB1 is related to tumor aggression in various human cancers (Kohno *et al.* 2003). We showed that ectopic expression of YB1 repressed *p16* transcription and resulted in the repression of cellular senescence. Cellular senescence functions as a barrier to hyperproliferation by oncogenic signals, such as the activation of Ras, and is achieved by *p16* induction (Serrano *et al.* 1997; Brookes *et al.* 2002; Braig *et al.* 2005; Collado *et al.* 2005). We postulate that YB1 up-regulation causes *p16* repression, thus resulting in the repression of cellular senescence. The implication is that this might contribute to the progression of various cancers.

Experimental procedures

Cell culture and senescence-associated expression of β-galactosidase (SA-β-Gal) assay

Early passage WI38 (normal human fibroblasts) cells were purchased from the American Type Culture Collection (ATCC) and cultured in Dulbecco's modified Eagle's medium

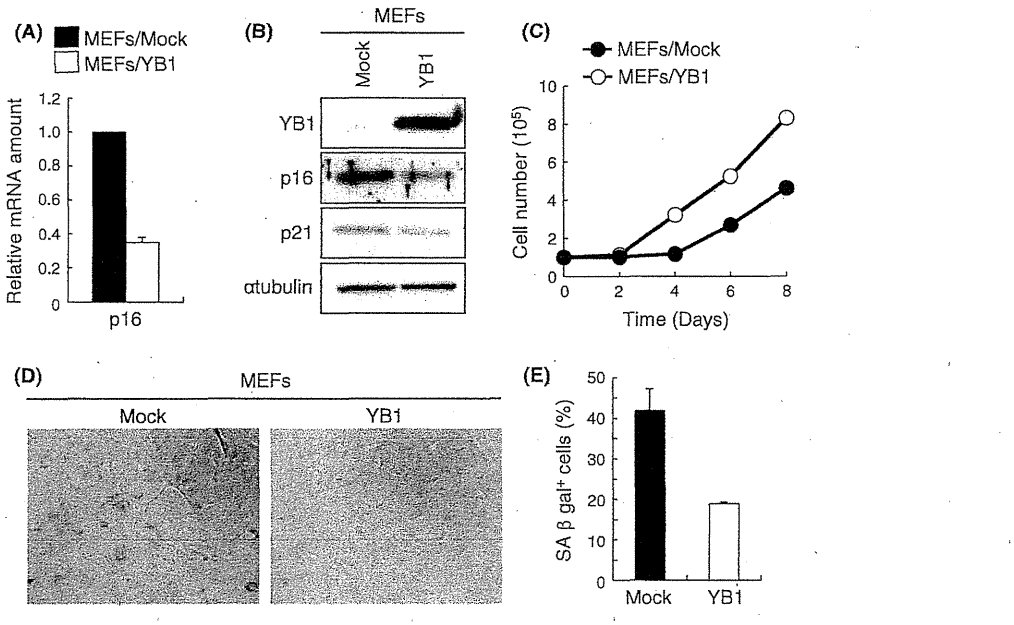

Figure 3 Ectopic expression of YB1 represses p16 expression in MEFs. (A, B) Early passage MEFs were infected with retroviruses expressing human YB1 or mock-infected as a control. Protein and mRNA quantification were determined by Western blotting and qRT-PCR, respectively. (C) The growth curves for MEFs infected with virus, or mock-infected, were determined by trypan blue staining. (D) MEFs stained for senescence-associated β-galactosidase (SA-β-gal) activity. (E) Proportion of SA-β-gal activity-positive cells.

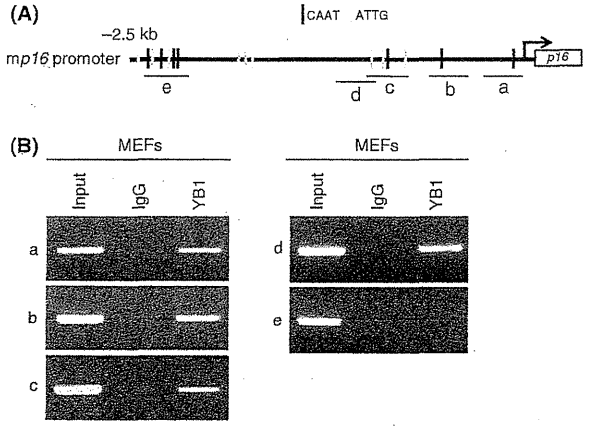

Figure 4 YB1 directly associated with the *p16* promoter region. (A) Schematic of potential YB1 binding sites and amplicons (a, b, c and d) used for ChIP assays targeting the mouse *p16* locus. (B) The binding of YB1 to the mouse *p16* promoter was determined by ChIP assay using IgG and an antibody against YB1. PCR was carried out using for each amplicon.

(DMEM) supplemented with 10% fetal bovine serum (FBS). Primary MEFs were isolated on embryonic day 13.5 (E13.5) and cultured as previously described (Nakayama *et al.* 1996). The SA-β-Gal assays were conducted using a Senescence Detection Kit (BioVision), according to the manufacturer's protocol. Briefly, MEFs were seeded to a 60% confluency in 6-well plates. The next day, the cells were washed with PBS and fixed with 1 mL of fixative solution provided with the kit for 10 min at room temperature. After washing with PBS, the cells were treated with 1 mL of the staining solution mix provided with the kit for overnight at 37 °C and then observed under a microscope.

Retroviral transduction

Human YB1 and H-Ras^{G12V} (kindly provided by C J Der, University of North Carolina at Chapel Hill, Chapel Hill, NC, USA) cDNAs were cloned into a pMX-puro retrovirus vector (kindly provided by T Kitamura, The University of Tokyo, Tokyo, Japan). Retroviral production was conducted as previously described (Kotake *et al.* 2007). Cells were infected with virus for 24 h and then treated again with virus-containing supernatant to increase infection efficiency. After infection, cells were selected using 2 μg/mL puromycin for 3 days.

Western blot

Western blot analysis was carried out as previously described (Kotake *et al.* 2007). Cells were lysed with RIPA buffer

(50 mM Tris–HCl pH 8.0, 150 mM NaCl, 1% NP-40, 0.5% DOC, 0.1% SDS, 1 mM Na_3VO_4, 1 mM DTT, 1 mM PMSF) supplemented with protease inhibitors (10 mg/L antipain, 10 mg/L leupeptin, 10 mg/L pepstatin, 10 mg/L trypsin inhibitor, 10 mg/L E64 and 2.5 mg/L chymostatin). The antibodies we used included anti-mouse p16 (M-156; Santa Cruz Biotechnology), anti-human p16 (ab50282; Abcam,), anti-mouse p21 (F-5; Santa Cruz Biotechnology), anti-p15 (Cell Signaling), anti-H-Ras (OP23; Calbiochem), anti-YB1 (ab12148; Abcam) and anti-α-tubulin (Sigma).

Quantitative reverse transcription polymerase chain reaction (qRT-PCR)

Total RNA was extracted using an RNeasy Plus kit (Qiagen), with 1 μg of total RNA applied to RT reactions that contained oligo$(dT)_{20}$ primers and SuperScript Reverse Transcriptase II (Invitrogen). The produced cDNA was added to a qRT-PCR mixture that contained 1 × SYBR Green PCR master mix (Qiagen) and 200 nM gene-specific primers. The expression level of each gene was normalized to a reference gene, glyceraldehyde-3-phosphate dehydrogenase (GAPDH). Assays were carried out in triplicate on an Mx3000P Real-Time Q-PCR System (Agilent Technologies) and Rotor-Gene 3000 system (Corbett Research). Primer sequences are available upon request.

RNA interference (RNAi)

The MEFs and WI38 cells were transfected with siRNA oligonucleotides using Lipofectamine RNAiMAX (Invitrogen), according to the manufacturer's protocol. The nucleotide sequences of siRNA for *YB1* were mouse, 5′-CAA CGU CGG UAU CGC CGA AAC UUC A-3′; and human, 5′-GGU UCC CAC CUU ACU ACER U-3′ with 3′ dTdT overhangs.

Chromatin immunoprecipitation (ChIP) assay

ChIP assays were carried out as previous described (Kotake *et al.* 2007). Approximately 3 × 10^6 MEFs were fixed with 1% formaldehyde for 10 min before 125 mM glycine was added. Cells were lysed in a lysis buffer (10 mM HEPES pH 7.9, 0.5% NP-40, 1.5 mM $MgCl_2$, 10 mM KCl, 0.5 mM DTT and protease inhibitor cocktail) on ice for 10 min and then centrifuged. Cell pellets were lysed in nuclear lysis buffer (20 mM HEPES pH 7.9, 25% glycerol, 0.5% NP-40, 0.42 M NaCl, 1.5 mM $MgCl_2$, 0.2 mM EDTA and protease inhibitor cocktail), sonicated and centrifuged. Lysates were diluted with an equal volume of dilution buffer (1% Triton X-100, 2 mM EDTA, 50 mM NaCl, 20 mM Tris–HCl pH 7.9, and protease inhibitor cocktail). Immunoprecipitation was conducted with a specific antibody against YB1 (RN015P; MBL). Normal rabbit IgG was used as a control. DNA fragments were purified with a PCR purification kit (Qiagen), and PCR was carried out using Platinum Taq polymerase (Invitrogen). The following primer pairs were used to amplify mouse *p16* fragments: (i), 5′-ACG TGT GCA CTT CTT TGC TG-3′ and 5′-CAT AGG TGG CGC TAT TTG C-3′; (ii), 5′-CCC TCC AAA ATG AGT TGT TTG-3′ and 5′-CTG GTC ACC CTT TGA CAC G-3′; (iii), 5′-GAG GCA GAA GGG AGA CAG AG-3′ and 5′-AAG TCA TCG GAG GGC AAT C-3′; (iv), 5′-TCG TGG AGT TGG TAA ATG AGG-3′ and 5′-TCC TCA CCA GAA AGG CAA TG-3′; and (v), 5′-GGA AAG CCC TGC AAT TTA CTC-3′ and 5′-CCC TTA TGG AGT CGA TTT TCC-3′.

Acknowledgements

We thank Yuuki Yasunaga and Mika Matsumoto for sample preparation and Dr. Kingo Chida and our laboratory members for helpful discussions. We also thank Professor Dr. Tetsuaki Nishida and Professor Dr. Masayuki Fujii, Kinki University, for their encouragement through this study and helpful discussions. This work was supported in part by grants from the Ministry of Education, Culture, Sports, Science and Technology of Japan 24700975 (Y. Kotake), 22300329 (M. Kitagawa), 24570151 (K. Kitagawa) and 23131504 (H. Niida) and from Iizuka City (Y. Kotake).

References

Asakuno, K., Kohno, K., Uchiumi, T., Kubo, T., Sato, S., Isono, M. & Kuwano, M. (1994) Involvement of a DNA binding protein, MDR-NF1/YB-1, in human MDR1 gene expression by actinomycin D. *Biochem. Biophys. Res. Commun.* **199**, 1428–1435.

Bargou, R.C., Jurchott, K., Wagener, C., Bergmann, S., Metzner, S., Bommert, K., Mapara, M.Y., Winzer, K.J., Dietel, M., Dorken, B. & Royer, H.D. (1997) Nuclear localization and increased levels of transcription factor YB-1 in primary human breast cancers are associated with intrinsic MDR1 gene expression. *Nat. Med.* **3**, 447–450.

Basaki, Y., Taguchi, K., Izumi, H., Murakami, Y., Kubo, T., Hosoi, F., Watari, K., Nakano, K., Kawaguchi, H., Ohno, S., Kohno, K., Ono, M. & Kuwano, M. (2010) Y-box binding protein-1 (YB-1) promotes cell cycle progression through CDC6-dependent pathway in human cancer cells. *Eur. J. Cancer* **46**, 954–965.

Bergmann, S., Royer-Pokora, B., Fietze, E., Jurchott, K., Hildebrandt, B., Trost, D., Leenders, F., Claude, J.C., Theuring, F., Bargou, R., Dietel, M. & Royer, H.D. (2005) YB-1 provokes breast cancer through the induction of chromosomal instability that emerges from mitotic failure and centrosome amplification. *Cancer Res.* **65**, 4078–4087.

Bracken, A.P., Kleine-Kohlbrecher, D., Dietrich, N., Pasini, D., Gargiulo, G., Beekman, C., Theilgaard-Monch, K., Minucci, S., Porse, B.T., Marine, J.C., Hansen, K.H. & Helin, K. (2007) The Polycomb group proteins bind throughout the INK4A-ARF locus and are disassociated in senescent cells. *Genes Dev.* **21**, 525–530.

Braig, M., Lee, S., Loddenkemper, C., Rudolph, C., Peters, A.H., Schlegelberger, B., Stein, H., Dorken, B., Jenuwein, T. & Schmitt, C.A. (2005) Oncogene-induced senescence as an initial barrier in lymphoma development. *Nature* **436**, 660–665.

Brookes, S., Rowe, J., Ruas, M., Llanos, S., Clark, P.A., Lomax, M., James, M.C., Vatcheva, R., Bates, S., Vousden, K.H., Parry, D., Gruis, N., Smit, N., Bergman, W. & Peters, G. (2002) INK4a-deficient human diploid fibroblasts are resistant to RAS-induced senescence. *EMBO J.* **21**, 2936–2945.

Cobrinik, D. (2005) Pocket proteins and cell cycle control. *Oncogene* **24**, 2796–2809.

Collado, M., Gil, J., Efeyan, A., Guerra, C., Schuhmacher, A.J., Barradas, M., Benguria, A., Zaballos, A., Flores, J.M., Barbacid, M., Beach, D. & Serrano, M. (2005) Tumour biology: senescence in premalignant tumours. *Nature* **436**, 642.

Fujii, T., Kawahara, A., Basaki, Y., Hattori, S., Nakashima, K., Nakano, K., Shirouzu, K., Kohno, K., Yanagawa, T., Yamana, H., Nishio, K., Ono, M., Kuwano, M. & Kage, M. (2008) Expression of HER2 and estrogen receptor alpha depends upon nuclear localization of Y-box binding protein-1 in human breast cancers. *Cancer Res.* **68**, 1504–1512.

Gil, J. & Peters, G. (2006) Regulation of the INK4b-ARF-INK4a tumour suppressor locus: all for one or one for all. *Nat. Rev. Mol. Cell Biol.* **7**, 667–677.

Gimenez-Bonafe, P., Fedoruk, M.N., Whitmore, T.G., Akbari, M., Ralph, J.L., Ettinger, S., Gleave, M.E. & Nelson, C.C. (2004) YB-1 is upregulated during prostate cancer tumor progression and increases P-glycoprotein activity. *Prostate* **59**, 337–349.

Gu, C., Oyama, T., Osaki, T., Kohno, K. & Yasumoto, K. (2001) Expression of Y box-binding protein-1 correlates with DNA topoisomerase IIalpha and proliferating cell nuclear antigen expression in lung cancer. *Anticancer Res.* **21**, 2357–2362.

Kim, W.Y. & Sharpless, N.E. (2006) The regulation of INK4/ARF in cancer and aging. *Cell* **127**, 265–275.

Kohno, K., Izumi, H., Uchiumi, T., Ashizuka, M. & Kuwano, M. (2003) The pleiotropic functions of the Y-box-binding protein, YB-1. *BioEssays* **25**, 691–698.

Kotake, Y., Cao, R., Viatour, P., Sage, J., Zhang, Y. & Xiong, Y. (2007) pRB family proteins are required for H3K27 trimethylation and Polycomb repression complexes binding to and silencing p16INK4alpha tumor suppressor gene. *Genes Dev.* **21**, 49–54.

Kotake, Y., Nakagawa, T., Kitagawa, K., Suzuki, S., Liu, N., Kitagawa, M. & Xiong, Y. (2011) Long non-coding RNA ANRIL is required for the PRC2 recruitment to and silencing of p15(INK4B) tumor suppressor gene. *Oncogene* **30**, 1956–1962.

Kotake, Y., Zeng, Y. & Xiong, Y. (2009) DDB1-CUL4 and MLL1 mediate oncogene-induced p16INK4a activation. *Cancer Res.* **69**, 1809–1814.

Krimpenfort, P., Quon, K.C., Mooi, W.J., Loonstra, A. & Berns, A. (2001) Loss of p16Ink4a confers susceptibility to metastatic melanoma in mice. *Nature* **413**, 83–86.

Lee, C., Dhillon, J., Wang, M.Y., Gao, Y., Hu, K., Park, E., Astanehe, A., Hung, M.C., Eirew, P., Eaves, C.J. & Dunn, S.E. (2008) Targeting YB-1 in HER-2 overexpressing breast cancer cells induces apoptosis via the mTOR/STAT3 pathway and suppresses tumor growth in mice. *Cancer Res.* **68**, 8661–8666.

Lu, Z.H., Books, J.T. & Ley, T.J. (2005) YB-1 is important for late-stage embryonic development, optimal cellular stress responses, and the prevention of premature senescence. *Mol. Cell. Biol.* **25**, 4625–4637.

Nakayama, K., Ishida, N., Shirane, M., Inomata, A., Inoue, T., Shishido, N., Horii, I. & Loh, D.Y. (1996) Mice lacking p27(Kip1) display increased body size, multiple organ hyperplasia, retinal dysplasia, and pituitary tumors. *Cell* **85**, 707–720.

Ohga, T., Koike, K., Ono, M., Makino, Y., Itagaki, Y., Tanimoto, M., Kuwano, M. & Kohno, K. (1996) Role of the human Y box-binding protein YB-1 in cellular sensitivity to the DNA-damaging agents cisplatin, mitomycin C, and ultraviolet light. *Cancer Res.* **56**, 4224–4228.

Ohtani, N., Zebedee, Z., Huot, T.J., Stinson, J.A., Sugimoto, M., Ohashi, Y., Sharrocks, A.D., Peters, G. & Hara, E. (2001) Opposing effects of Ets and Id proteins on p16INK4a expression during cellular senescence. *Nature* **409**, 1067–1070.

Okamoto, T., Izumi, H., Imamura, T., Takano, H., Ise, T., Uchiumi, T., Kuwano, M. & Kohno, K. (2000) Direct interaction of p53 with the Y-box binding protein, YB-1: a mechanism for regulation of human gene expression. *Oncogene* **19**, 6194–6202.

Ruas, M. & Peters, G. (1998) The p16INK4a/CDKN2A tumor suppressor and its relatives. *Biochim. Biophys. Acta* **1378**, F115–F177.

Serrano, M., Hannon, G.J. & Beach, D. (1993) A new regulatory motif in cell-cycle control causing specific inhibition of cyclin D/CDK4. *Nature* **366**, 704–707.

Serrano, M., Lin, A.W., McCurrach, M.E., Beach, D. & Lowe, S.W. (1997) Oncogenic ras provokes premature cell senescence associated with accumulation of p53 and p16INK4a. *Cell* **88**, 593–602.

Sharpless, N.E. (2005) INK4a/ARF: a multifunctional tumor suppressor locus. *Mutat. Res.* **576**, 22–38.

Sharpless, N.E., Bardeesy, N., Lee, K.H., Carrasco, D., Castrillon, D.H., Aguirre, A.J., Wu, E.A., Horner, J.W. & DePinho, R.A. (2001) Loss of p16Ink4a with retention of p19Arf predisposes mice to tumorigenesis. *Nature* **413**, 86–91.

Sherr, C.J. (2006) Divorcing ARF and p53: an unsettled case. *Nat. Rev. Cancer* **6**, 663–673.

Shibahara, K., Sugio, K., Osaki, T., Uchiumi, T., Maehara, Y., Kohno, K., Yasumoto, K., Sugimachi, K. & Kuwano, M. (2001) Nuclear expression of the Y-box binding protein, YB-1, as a novel marker of disease progression in non-small cell lung cancer. *Clin. Cancer Res.* **7**, 3151–3155.

Shibao, K., Takano, H., Nakayama, Y., Okazaki, K., Nagata, N., Izumi, H., Uchiumi, T., Kuwano, M., Kohno, K. & Itoh, H. (1999) Enhanced coexpression of YB-1 and DNA topoisomerase II alpha genes in human colorectal carcinomas. *Int. J. Cancer* **83**, 732–737.

Sorokin, A.V., Selyutina, A.A., Skabkin, M.A., Guryanov, S.G., Nazimov, I.V., Richard, C., Th'ng, J., Yau, J., Sorensen, P.H., Ovchinnikov, L.P. & Evdokimova, V. (2005) Proteasome-mediated cleavage of the Y-box-binding protein 1 is linked to DNA-damage stress response. *EMBO J.* **24**, 3602–3612.

Uchiumi, T., Fotovati, A., Sasaguri, T., Shibahara, K., Shimada, T., Fukuda, T., Nakamura, T., Izumi, H., Tsuzuki, T., Kuwano, M. & Kohno, K. (2006) YB-1 is important for an early stage embryonic development: neural tube formation and cell proliferation. *J. Biol. Chem.* **281**, 40440–40449.

Wu, J., Lee, C., Yokom, D., Jiang, H., Cheang, M.C., Yorida, E., Turbin, D., Berquin, I.M., Mertens, P.R., Iftner, T., Gilks, C.B. & Dunn, S.E. (2006) Disruption of the Y-box binding protein-1 results in suppression of the epidermal growth factor receptor and HER-2. *Cancer Res.* **66**, 4872–4879.

Yap, K.L., Li, S., Munoz-Cabello, A.M., Raguz, S., Zeng, L., Mujtaba, S., Gil, J., Walsh, M.J. & Zhou, M.M. (2010) Molecular interplay of the noncoding RNA ANRIL and methylated histone H3 lysine 27 by polycomb CBX7 in transcriptional silencing of INK4a. *Mol. Cell* **38**, 662–674.

Received: 18 June 2013
Accepted: 7 August 2013.

Supporting Information

Additional Supporting Information may be found in the online version of this article at the publisher's web site:

Figure S1 YB1 binds to the mouse *p16* promoter.

Cell. Mol. Life Sci. (2013) 70:4785–4794
DOI 10.1007/s00018-013-1423-0

Cellular and Molecular Life Sciences

REVIEW

Cell cycle regulation by long non-coding RNAs

Masatoshi Kitagawa · Kyoko Kitagawa · Yojiro Kotake · Hiroyuki Niida · Tatsuya Ohhata

Received: 21 March 2013 / Revised: 24 June 2013 / Accepted: 4 July 2013 / Published online: 24 July 2013

Abstract The mammalian cell cycle is precisely controlled by cyclin-dependent kinases (CDKs) and related pathways such as the RB and p53 pathways. Recent research on long non-coding RNAs (lncRNAs) indicates that many lncRNAs are involved in the regulation of critical cell cycle regulators such as the cyclins, CDKs, CDK inhibitors, pRB, and p53. These lncRNAs act as epigenetic regulators, transcription factor regulators, post-transcription regulators, and protein scaffolds. These cell cycle-regulated lncRNAs mainly control cellular levels of cell cycle regulators via various mechanisms, and may provide diversity and reliability to the general cell cycle. Interestingly, several lncRNAs are induced by DNA damage and participate in cell cycle arrest or induction of apoptosis as DNA damage responses. Therefore, deregulations of these cell cycle regulatory lncRNAs may be involved in tumorigenesis, and they are novel candidate molecular targets for cancer therapy and diagnosis.

Keywords lncRNA · DNA damage response · Cyclin-CDK · CDK inhibitor · pRB · p53

M. Kitagawa (✉) · K. Kitagawa · Y. Kotake · H. Niida · T. Ohhata
Department of Molecular Biology, Hamamatsu University School of Medicine, 1-20-1 Handayama, Higashi-ku, Hamamatsu 431-3125, Japan
e-mail: kitamasa@hama-med.ac.jp

Y. Kotake
Department of Biological and Environmental Chemistry, Faculty of Humanity-Oriented Science and Engineering, Kinki University, 11-6 Kayanomori, Iizuka, Fukuoka 820-8555, Japan

Introduction

The mammalian cell cycle is controlled by cyclin-dependent kinases (CDKs) and their related pathways (Fig. 1) [1, 2]. The CDKs, particularly CDK1, CDK2, and CDK4/6, are activated via binding to their selected cyclins, including cyclins A, B, D, and E, in specific phases of the cell cycle, following which they phosphorylate their target proteins to enable cell cycle progression. The activities of the CDKs are controlled not only by cyclins but also by phosphorylation or dephosphorylation by Wee1 kinase or CDC25 phosphatase [1]. Moreover, CDK inhibitors including $p15^{ink4b}$, $p16^{ink4a}$, $p18^{ink4d}$, $p21^{Cip1}$, $p27^{Kip1}$, and $p57^{Kip2}$ specifically bind to their target cyclin–CDK complexes and inhibit their activities to negatively regulate the cell cycle [3–5].

CDKs and their related pathways control the cell cycle by maintaining exit and entry to the different phases of the cell cycle. In the G1 phase, growth stimuli such as growth factors often activate the MAP kinase pathway, following which genes encoding the cyclin Ds are transcribed. The resulting products bind to and activate CDK4/6 [6]. Cyclin Ds–CDK4/6 complexes phosphorylate retinoblastoma protein (pRB) and its family members, p107 and p130, in the late G1 phase and activate E2F-mediated transcription, which induces the expression of several growth-promoting genes [7, 8]. At the G1/S transition point, cyclin E-CDK2 phosphorylates pRB as well as several proteins involved in DNA replication to promote G1/S progression [9]. Cyclin B-CDK1 has many targets including APC/cyclosome, and promotes maturation of the G2 phase and critically participates in M phase events [10].

The cellular levels of cell cycle regulators such as cyclins, CDKs, CDK inhibitors, CDC25, RB, and E2F are critical for cell cycle regulation. After the cell cycle regulators complete their functions, they are ubiquitylated by

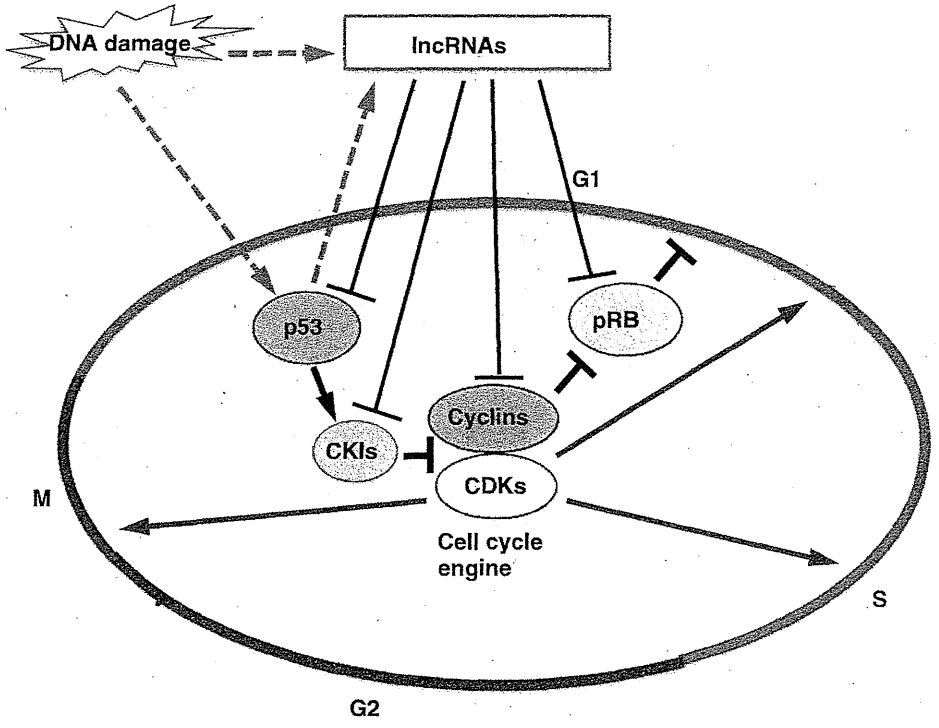

Fig. 1 Outline of cell cycle control and involvement of lncRNAs. The mammalian cell cycle is controlled by cyclin-dependent kinases (CDKs) and their related pathways. CDKs are activated via binding to their selected cyclins in specific phases of the cell cycle, following which they phosphorylate their target proteins. The CDK inhibitors (CKIs) negatively regulate the activities of CDKs and control the cell cycle. pRB regulates G1/S progression. The p53 pathway plays a role in DNA damage response as a gatekeeper of the genome. Several lncRNAs control the expression of cyclins-CDKs, CKIs, pRB and p53, and participate in cell cycle regulation. Some of these lncRNAs are induced by DNA damage and inhibit cell cycle progression by regulating these cell cycle regulators

specific E3 ligases and eliminated via the ubiquitin–proteasome pathway [11–13]. The level of cell cycle regulators is precisely controlled by not only post-translational but also translational mechanisms. For example, several micro-RNAs (miRNAs) participate in cell cycle regulation through translational regulation [14]. MiRNAs are small non-coding RNA molecules containing 22 nucleotides, and negatively regulate translation through binding of the untranslated region of its target mRNAs [15]. The let-7 miRNA family negatively regulates cyclins A and D, and CDK4/6 and CDC25A [16]. The miR-15 family also inhibits the translation of cyclin D, CDK4, and CDC27 [17, 18]. Interestingly, these let-7 and miR-15 family members may be involved in tumorigenesis since they are downregulated in various human cancers [16–18]. Alternatively, cyclin D1 is a target for not only let-7 and miR-15 miRNAs but also miR-19a, 26a, and 34a [15]. Furthermore, p27 ^{Kip1} is targeted for regulation by the miR-181 family [19] and the miR-221 family [20]. The roles of other miRNAs in the expression of cell cycle regulators have also been reported [15]. Thus, it has been shown that the cell cycle regulators are critically and precisely controlled by E3 ligases and miRNAs both post-translationally and at the translational level.

Here, we focus on long non-coding RNAs (lncRNAs) involved in the regulation of the cell cycle through their various functions as epigenetic regulators, transcription factor regulators, post-transcription regulators and protein scaffolds [21, 22]. LncRNAs are non-protein coding transcripts longer than 200 nucleotides, and can be divided into at least five categories based on their structural characteristics, including intergenic lncRNAs (lincRNAs), intronic lncRNAs, natural antisense transcripts, pseudogenes, and retrotransposons [23]. Recent mass-scale transcriptome analysis has revealed that many kinds of lncRNAs are transcribed in large amounts in the eukaryotic genome [24]. However, the question remains as to whether these lncRNAs are merely by-products of the transcriptional units or have a critical function for biological processes. However, it has become clear that some of these lncRNAs participate in various biological processes such as genome imprinting, X-inactivation, development, differentiation, and cell cycle regulation [22, 24–26]. For example, *HOTAIR*, a well-investigated lncRNA, is involved in correct development

Table 1 LncRNAs involved in the cell cycle control

lncRNA	How it is induced	The effects of the lncRNA on its targets in cell cycle (phase)	References
ncRNA$_{CCND1}$	DNA damage	Suppression of *Cyclin D1* transcription with TLS (G1)	[33, 34]
gadd7	DNA damage	Destabilization of *CDK6 mRNA* (G1)	[35, 36]
MALAT1	High expression In cancer	Promotion of cell-cycle regulators such as cyclin A2 and B1 (G1 and G2/M)	[37–39]
SRA	?	Suppression of *Cyclin A, B cdc20. Cdt1* transcription (G1 and G2/M)	[40, 41]
ANRIL	DNA damage	Suppression of *p15/p16* transcription with PRC1/2 (G1)	[31, 32, 52]
lncRNA-HEIH	High expression In HCC	Suppression of *p16. p21, p27 and p57* transcription with PRC2(G0/G1)	[53]
HULC	HBx-mediated	Suppression of *p18* expression (G1)	[60–62]
KCNQ10T1	Paternal expression	Suppression of *p57* transcription with PRC2 and G9a (G1?)	[64]
H19 lncRNA	E2F1-mediated	Downregulation of *RB mRNA* via *miR675* (G1)	[69–71]
lncRNA-RoR	p53-mediated	Suppression of *p53 mRNA* translation (G2/M)	[74]
p53-induced eRNA	p53-mediated	Promotion of p53 target genes transcription (G1?)	[75]
loc285194	p53-mediated	Growth inhibition by suppression of miR211 (G1?)	[76]
lncRNA-p21	p53-mediated	Suppression of transcription of the target genes involved in apoptosis and cell cycle with hnRNA-K (G1?) suppression of β-catenin and *Jun B mRNA* translation	[77, 78]
PANDA	DNA damage	Suppression of *FAS* and *BIK* transcription (G1?)	[79]

and tumorigenesis through recruiting the polycomb group (PcG) complex to its targeted *HOX* genes for their repression [26, 27]. The PcG complex contributes to the epigenetic regulation of its target genes by forming Polycomb repressive complex 1 (PRC1) and 2 (PRC2). PRC2 participates in histone H3K27 methylation and, following histone H2AK119 monoubiquitination by PRC1, collaboratively represses target gene transcription. In addition to *HOTAIR*, several lncRNAs such as *XIST*, *AIR*, and *KCNQ1OT1* also recruit chromatin modifiers including PcG and H3K9 methyltransferase G9a to their target loci [25, 28–30]. Moreover, *ANRIL* (antisense non-coding RNA in the *INK4* locus) directly binds to PcGs and recruits them to the *INK4* locus to promote gene silencing [31, 32]. Thus, *HOTAIR, XIST, AIR, KCNQ1OT1*, and *ANRIL* function as epigenetic regulators by negatively regulating target gene transcription through recruitment of chromatin modifiers. Recently, several lncRNAs that participate in the expression of several cell cycle regulators have been reported (summarized in Fig. 1; Table 1). In this review, we introduce these lncRNAs and discuss their functions in cell cycle regulation.

LncRNAs regulating cyclins and CDKs

Cyclins and CDKs are key players in cell cycle regulation (Fig. 1). *NcRNA$_{CCND1}$*, also called pncRNA (promoter-associated non-coding RNA), is transcribed from the upstream region of the *cyclin D1* gene, *CCND1*, and negatively regulates cyclin D1. *NcRNA$_{CCND1}$* functions as a transcription factor regulator [33]. It is induced in a DNA damage-dependent manner, and associates with and recruits TLS (translocated in liposarcoma) [34], an RNA binding protein. The *ncRNA$_{CCND1}$*-TLS complex is recruited to the *CCND1* promoter to inhibit the activity of the coactivator, CBP/p300, thereby preventing *CCND1* transcription (Fig. 2a). Thus, suppression of cyclin D1 regulated by the *ncRNA$_{CCND1}$*-TLS complex may participate in G1 arrest in response to DNA damage.

Gadd7 is an lncRNA involved in regulating CDK6 expression [35] in a posttranscriptional manner. TDP-43 (TAR DNA binding protein) binds to the 3′ untranslated region of *CDK6* mRNA to stabilize it. *Gadd7* is transcriptionally induced via DNA damage mediated by UV and cisplatin [35, 36], and binds to TDP-43 and dissociates from *CDK6* mRNA. The *CDK6* mRNA is then degraded, resulting in inhibition of the G1/S transition (Fig. 2b). Therefore, *gadd7* negatively controls CDK6 expression, functioning as a translation regulator. Interestingly, *gadd7* specifically controls mRNA stability for *CDK6*, but not *CDK4*, *CDK2*, or *CCND1*, by trapping TDP-43. The physiological relevance of the selective suppression of *CDK6* remains to be determined. *Gadd7* may be involved in the G1 checkpoint by collaborating with the lncRNA, *ncRNA$_{CCND1}$*, to downregulate the cyclin D1–CDK6 complex, thereby arresting cell cycle progression in response to DNA damage (Fig. 2a, b). This may represent a novel G1-checkpoint cascade, but further studies are required.

MALAT1, an mRNA splicing mediator [37], is upregulated in several human cancers and contributes to cancer cell proliferation [38]. *MALAT1* depletion results in arrest at G1 and promotes expression of p53 as well as p16, p21, and p27 in human fibroblasts [39] (Table 1). In contrast, *MALAT1* depletion suppresses various genes involved in

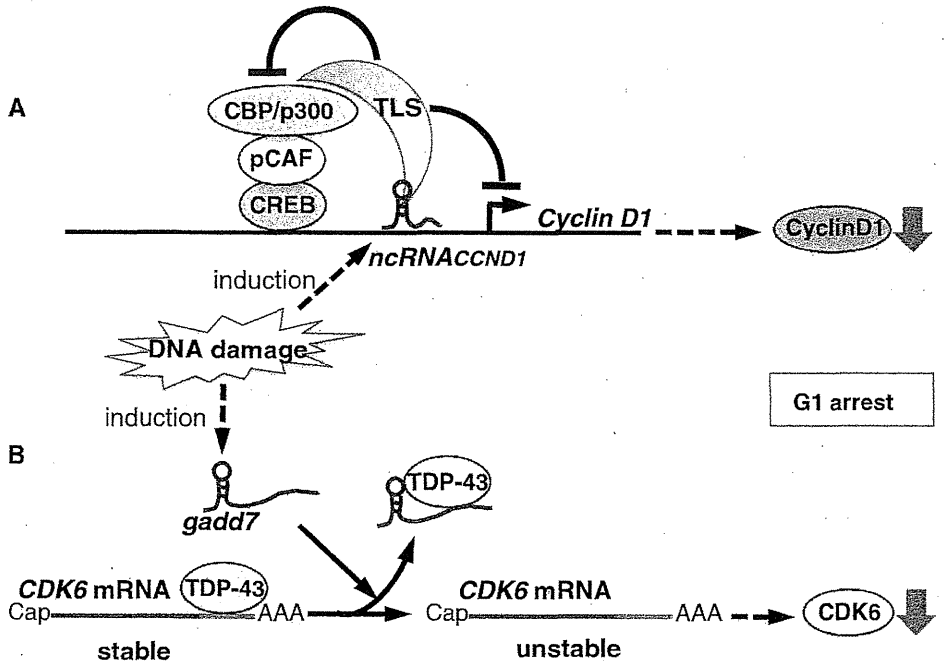

Fig. 2 Model showing the proposed mechanisms of lncRNA-mediated regulation of cyclin D1 (**a**) and CDK6 (**b**) induced by DNA damage. **a** DNA damage induces the transcription of $ncRNA_{CCND1}$ from the promoter region of the *cyclin D1* gene. $ncRNA_{CCND1}$ associates with and recruits TLS, an RNA binding protein, to the *cyclin D1* promoter. The $ncRNA_{CCND1}$–TLS complex inhibits the CBP/p300–pCAF–CREB coactivator complex and thereby prevents *cyclin D1* gene transcription. **b** DNA damage induces the expression of the lncRNA, *gadd7*, which dissociates TDP-43 from the CDK6 mRNA to destabilize it, and CDK6 is thereby downregulated, inhibiting the G1/S transition. The lncRNAs *gadd7* and $ncRNA_{CCND1}$ may collaboratively participate in the G1 checkpoint in response to DNA damage

cell cycle progression such as the genes encoding cyclin A2 and Cdc25A, thereby arresting the cell cycle in G1. Moreover, in G2/M progression, *MALAT1* is required for expression of B-Myb, which is involved in the expression of mitotic proteins such as cyclin B1, CDK1, FoxoM1, and PLK by controlling the splicing of B-Myb mRNA [39]. Therefore, *MALAT1* may contribute to cell cycle progression in each phase by coordinated control of cell cycle regulators.

Steroid receptor RNA activator (*SRA*) was identified as an lncRNA that binds to steroid receptors [40]. *SRA* forms the SRC-1 complex to activate transcription, mediated by steroid receptors such as progesterone receptor and estrogen receptor. It also binds to various other proteins such as myoD, and has multiple cellular functions such as myogenesis. *SRA* also binds to PPARγ and coactivates gene expression mediated by PPARγ. As such, *SRA* regulates adipogenesis and insulin sensitivity via PPARγ [41]. Additionally, *SRA* shows PPARγ-independent activity. Overexpression of *SRA* in pre-adipocytes downregulates the expression of cell cycle-promoting genes such as those encoding the cyclins [cyclins (A2, B1/2)], *CDC20*, *MCMs* (*3, 4, 5, 6*), and *CDT1*. Conversely, these genes are upregulated by depletion of *SRA*. However, it remains to be elucidated whether *SRA* directly or indirectly suppresses the transcription of these genes, and further investigation into the mechanisms of *SRA*-regulated gene expression is required.

LncRNAs regulating CDK inhibitors

INK4 family inhibitors

The CDK inhibitory proteins, $p16^{ink4a}$ and $p15^{ink4b}$ (hereafter p16 and p15), bind to and inhibit CDK4 and 6, respectively, via their ankyrin repeats [3, 42]. The p15 and p16 genes (*CDKN2B* and *CDKN2A*, respectively) are located at the *INK4* locus together with the alternating reading frame gene, *ARF* [42]. ARF inhibits MDM2-dependent degradation of both p53 [43] and pRB [44]. Therefore, the expression of *INK4* locus genes is critical for cell cycle regulation. The INK4 proteins are relatively stable, and their ubiquitin-dependent proteolysis is not particularly important for controlling their cellular levels. Therefore, the *INK4* locus genes are mainly regulated by transcription. The participation of several transcription factors, including the ETS family [45], FOXO [46], and SP1 [47], has been reported. Moreover, the locus is regulated epigenetically. It has been suggested that PU.1 cooperates with